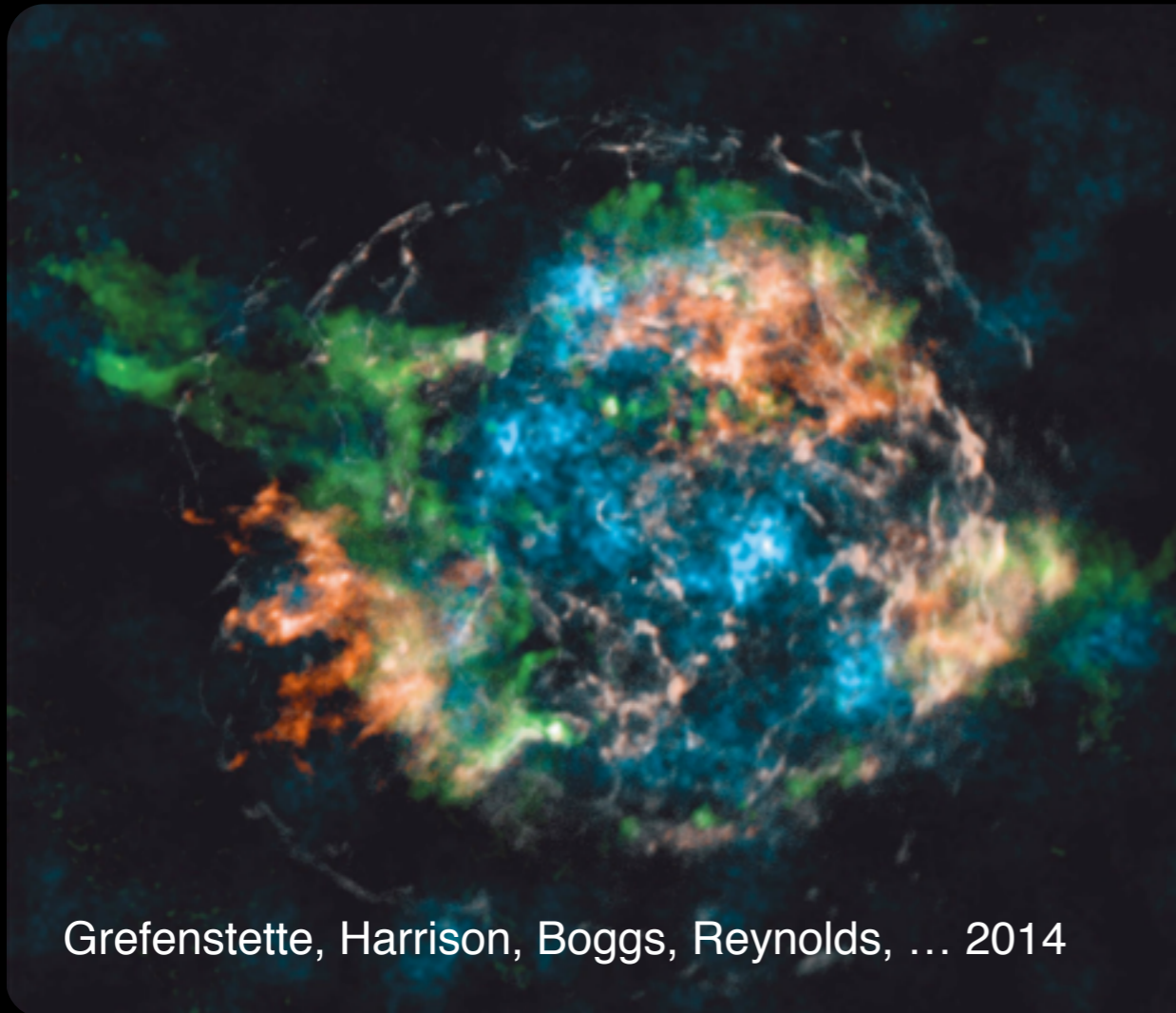
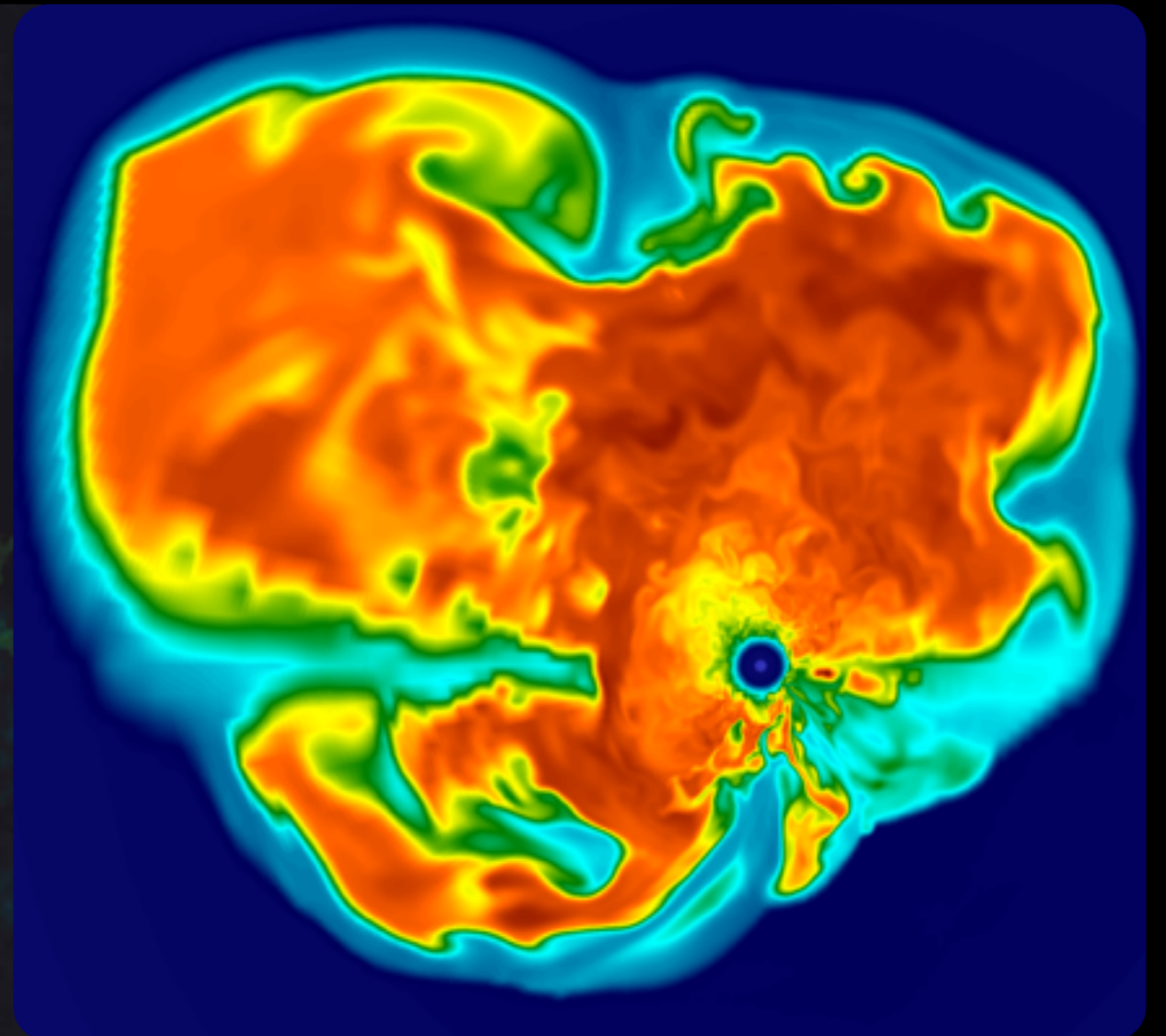


# MULTIDIMENSIONAL SIMULATIONS OF CORE-COLLAPSE SUPERNOVAE



Grefenstette, Harrison, Boggs, Reynolds, ... 2014

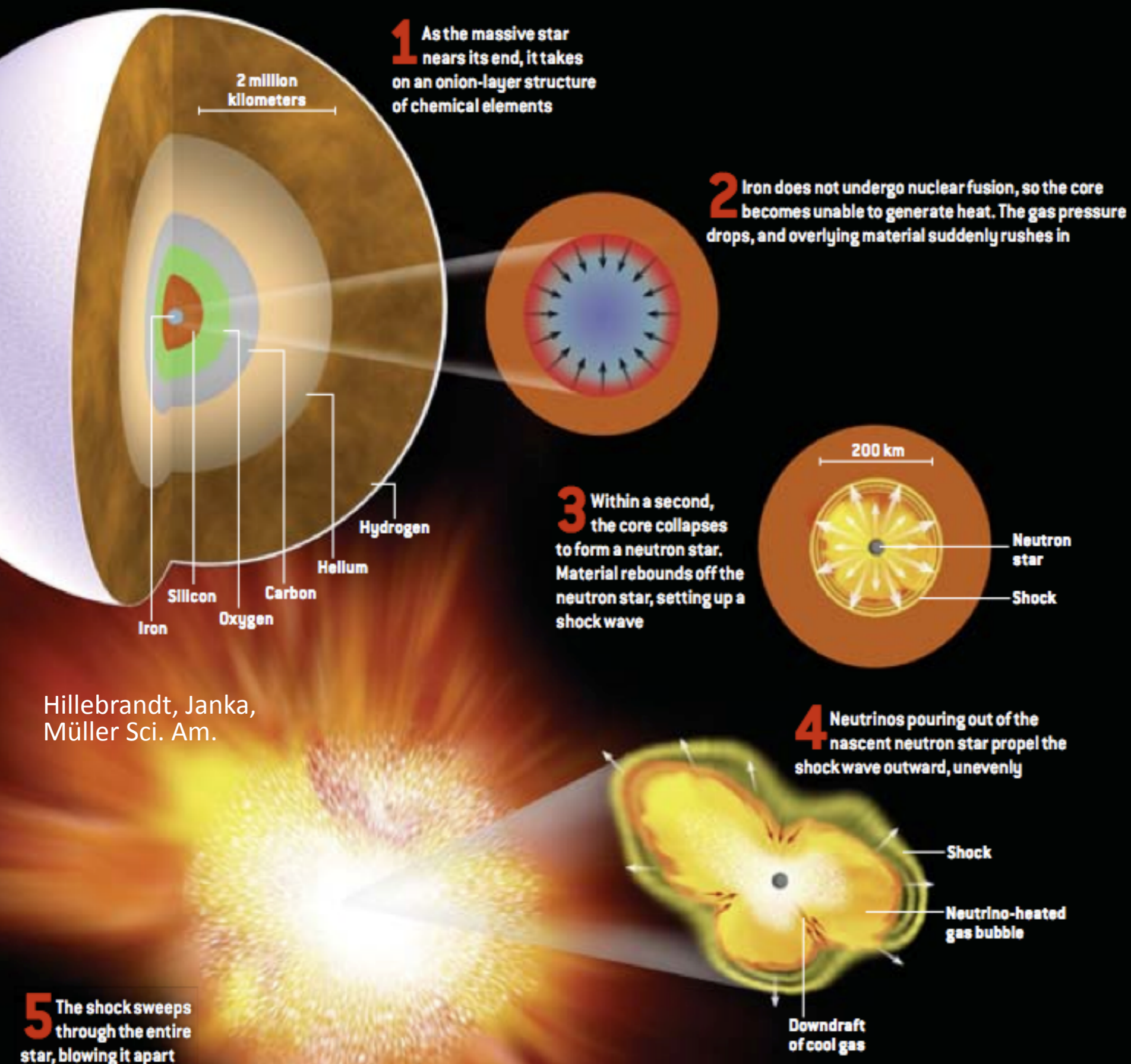


## & THEIR IMPACT ON SN NUCLEOSYNTHESIS

William Raphael Hix (ORNL/U. Tennessee)

*Blondin, Bruenn, Budiardja, Chertkow, Endeve, Fröhlich, Harris, Lee, Lentz, Marronetti, Mauney, Messer, Mezzacappa & Yakunin* (Florida Atlantic U., NC State U., ORNL/UT)

# TEXTBOOK SUPERNOVA



Hillebrandt, Janka,  
Müller Sci. Am.

A Core-Collapse Supernova is the **inevitable death** knell of a massive star ( $\sim 10+ M_{\odot}$ ).

The explosion enriches the interstellar medium with elements from **Oxygen to Nickel** and potentially the **r-process** elements as well.

# CHIMERA



CHIMERA has 3 “heads”

Spectral Neutrino Transport (MGFLD-TRANS, Bruenn)  
in **Ray-by-Ray Approximation**

Shock-capturing Hydrodynamics (VH1, Blondin)

Nuclear Kinetics (XNet, Hix & Thielemann)

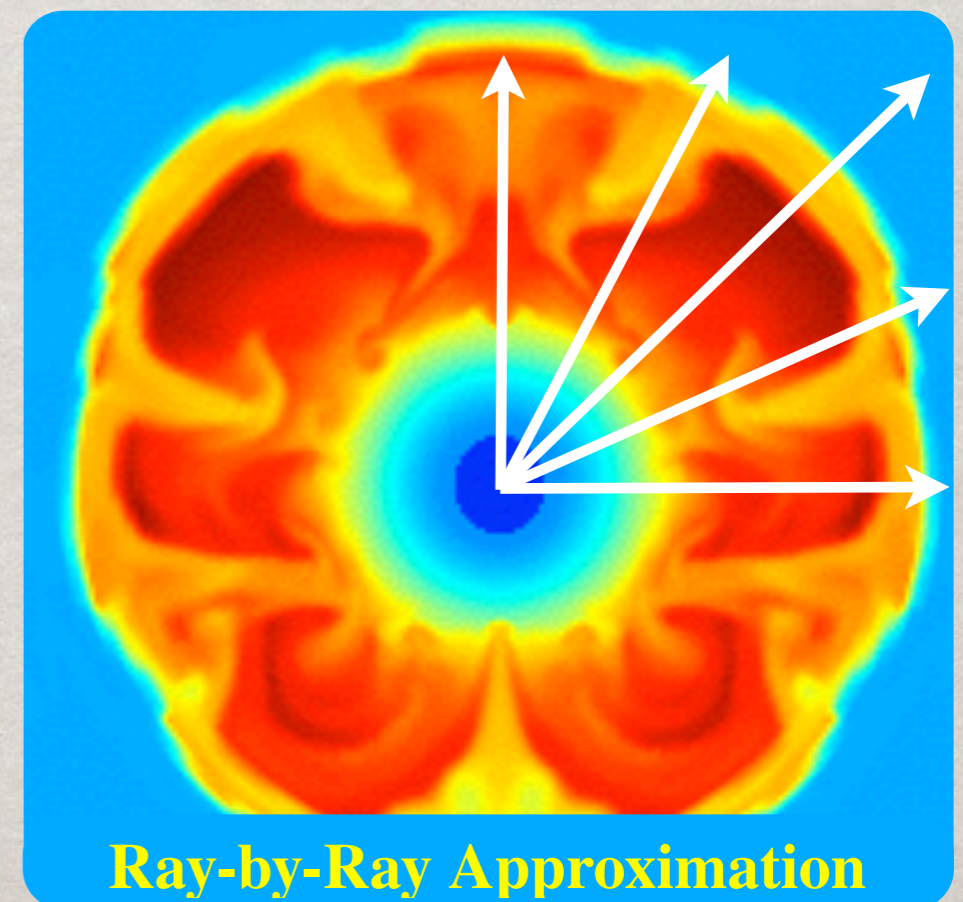
Plus Realistic Equations of State, Newtonian Gravity  
with Spherical GR Corrections.

Models use a variety of approximations

**Self-consistent** (*ab initio*) models use  
full physics to the center.

**Leakage** models simplify the transport.

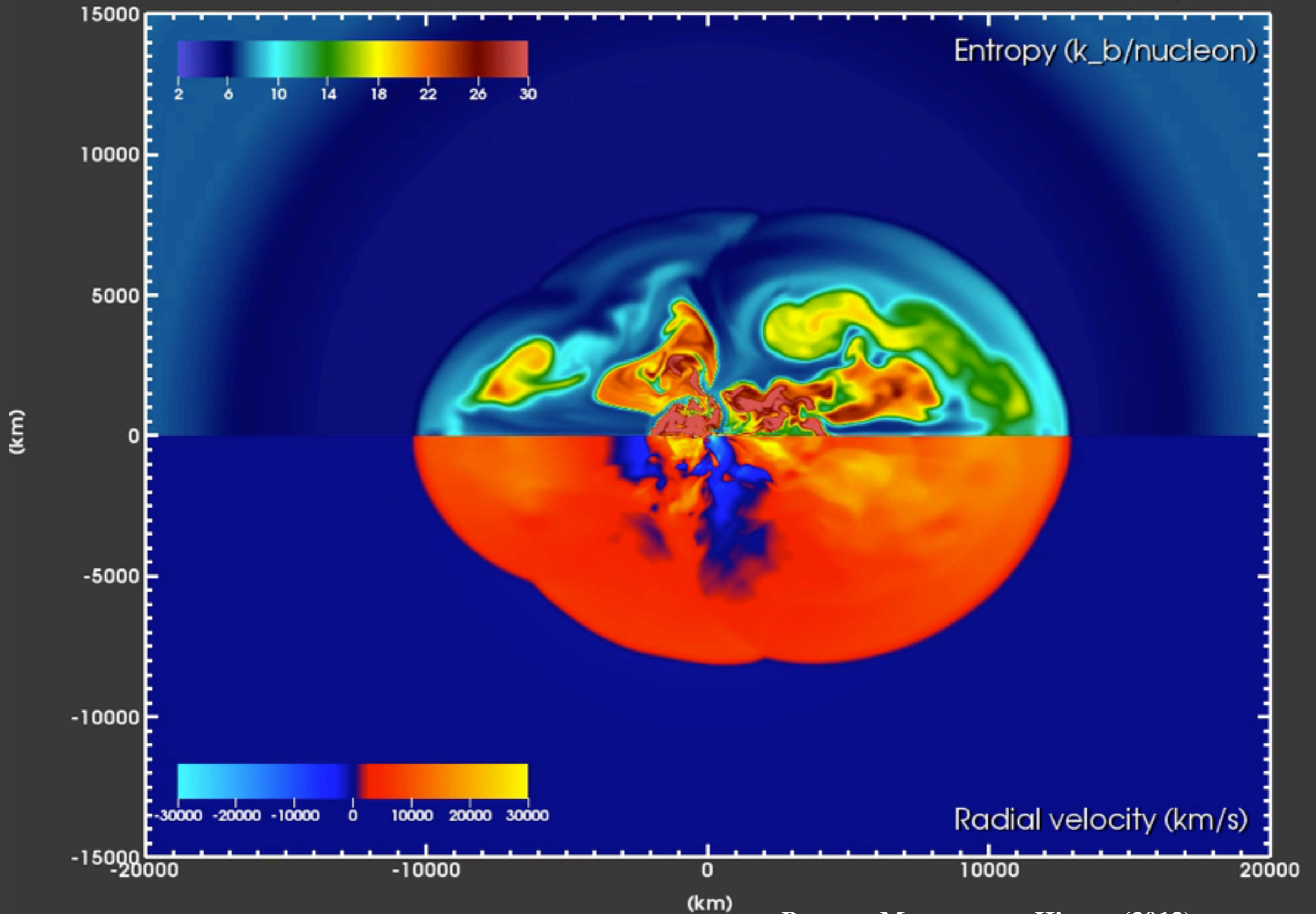
**Parameterized** models replace the core  
with a specified neutrino luminosity.



# SUPERNOVA: THE MOVIE

Chimera model: B12-WH07

1004.0 ms



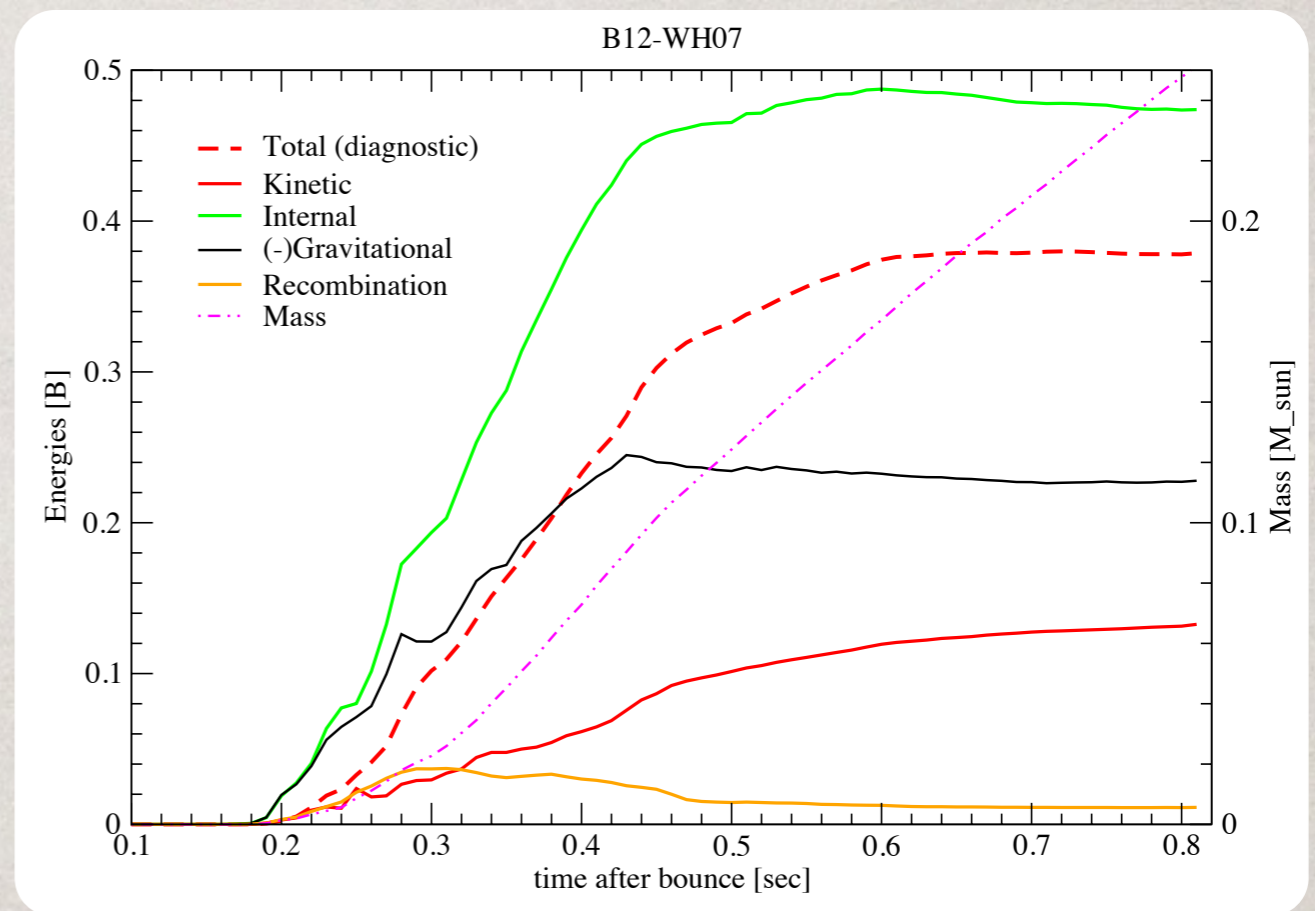
Bruenn, Mezzacappa, Hix, ... (2013)

# EXPLOSION ENERGIES

Once we achieve the most basic observable, an explosion, we can begin to compare to the myriad of other potential observations.

Foremost is the kinetic energy of the explosion.

Unfortunately, models are still in the stage where internal energy dominates, so we must estimate the explosion energy by assuming efficient conversion of  $E_i \Rightarrow E_k$ .

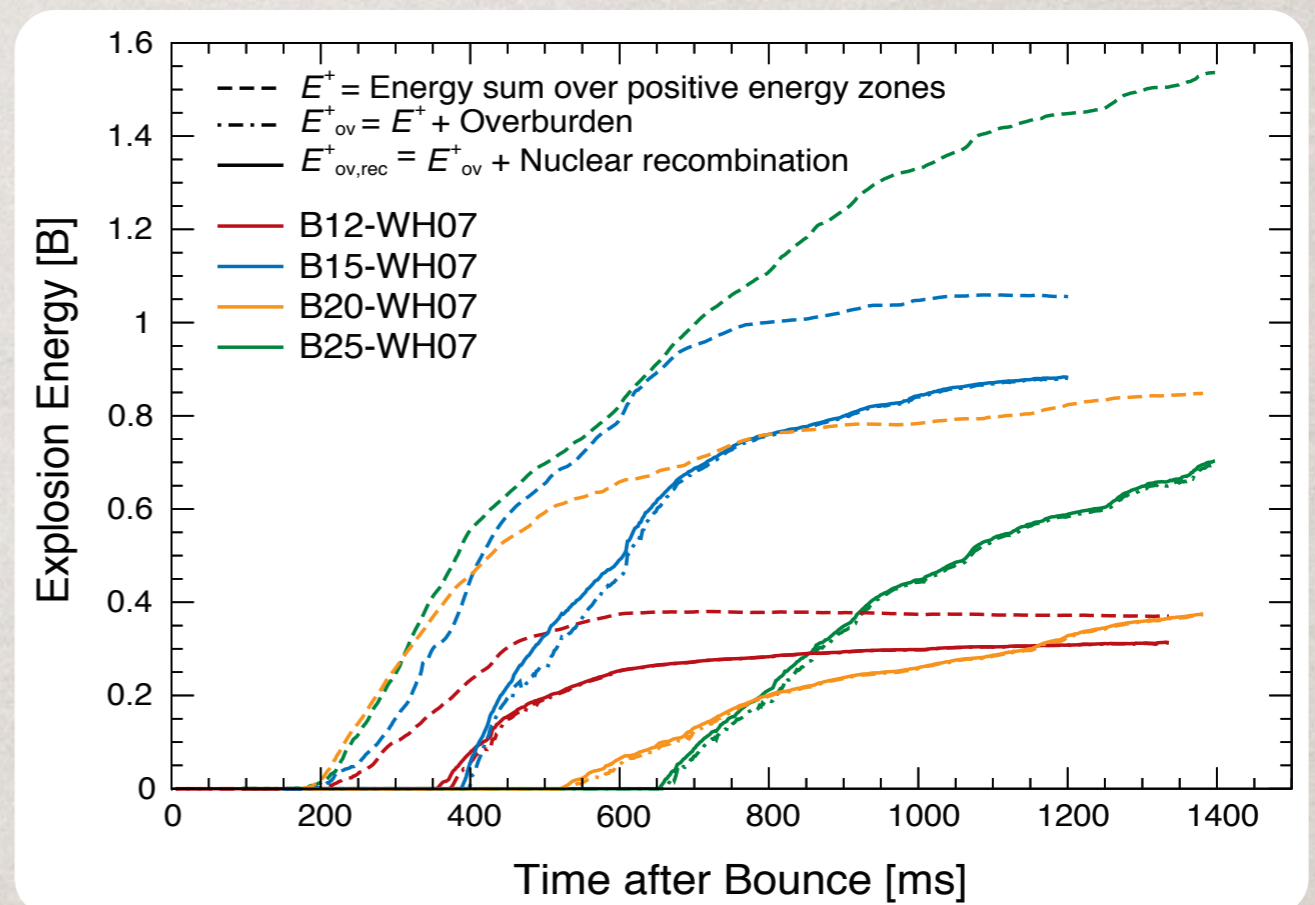
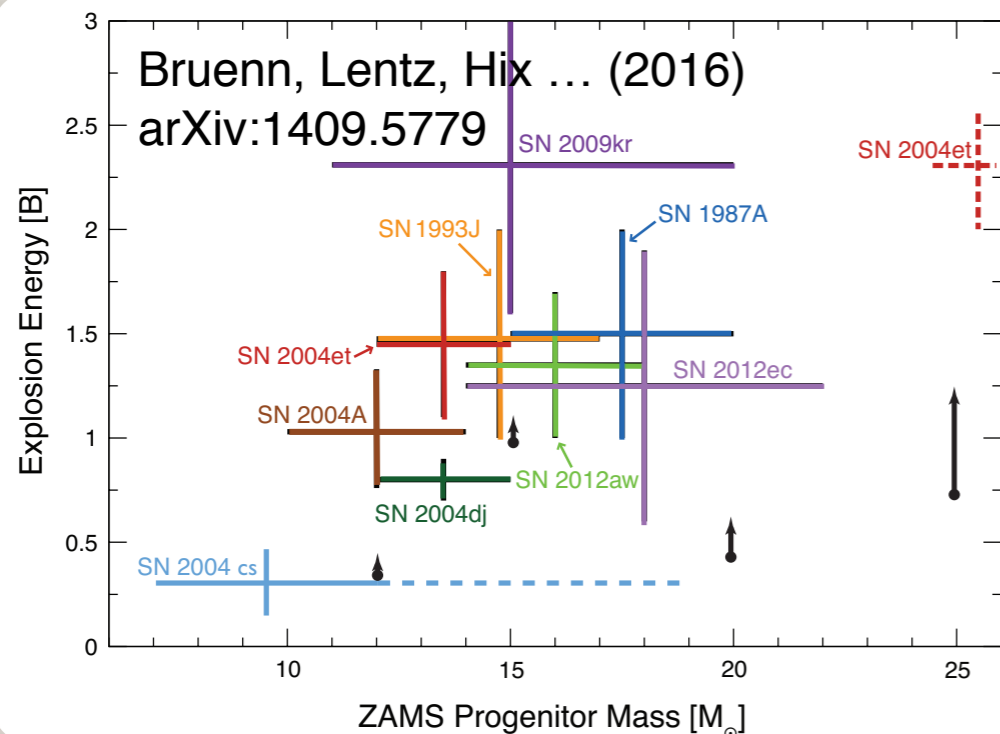


# EXPLOSION ENERGIES

Once we achieve the most basic observable, an explosion, we can begin to compare to the myriad of other potential observations.

Foremost is the kinetic energy of the explosion.

Unfortunately, models are still in the stage where internal energy dominates, so we must estimate the explosion energy by assuming efficient conversion of  $E_i \Rightarrow E_k$ .



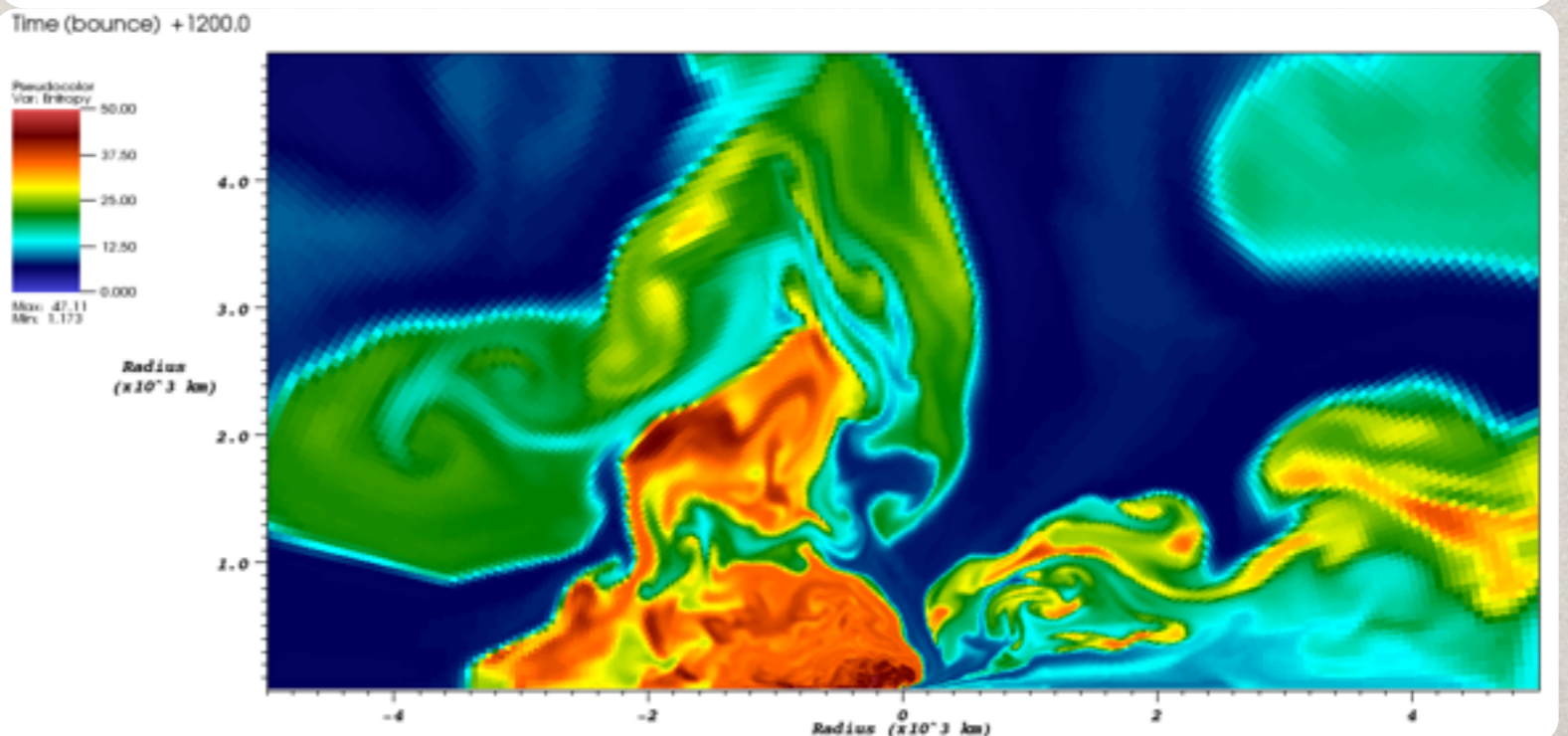
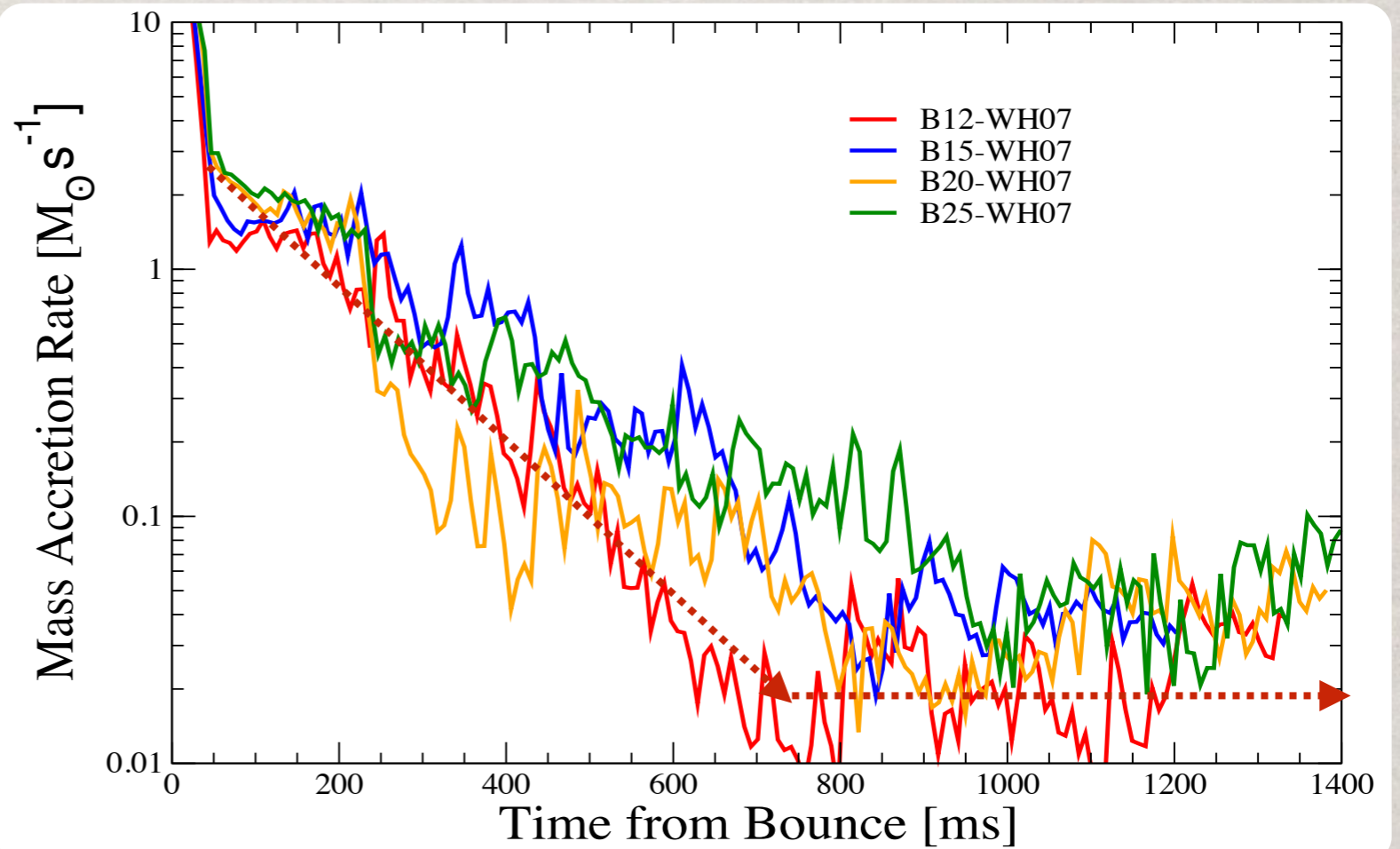
One can construct a “diagnostic” energy,  $E^+ = E_i + E_g + E_k$ , summed over zones where  $E^+ > 0$ .

To this we add contributions from nuclear recombination and removing the envelope.

# END OF THE EXPLOSION?

Even in our most fully developed model, the explosion energy **has not leveled off** 1.3 seconds after bounce.

The reason is that **accretion continues** at an appreciable rate, showing no sign of abating.

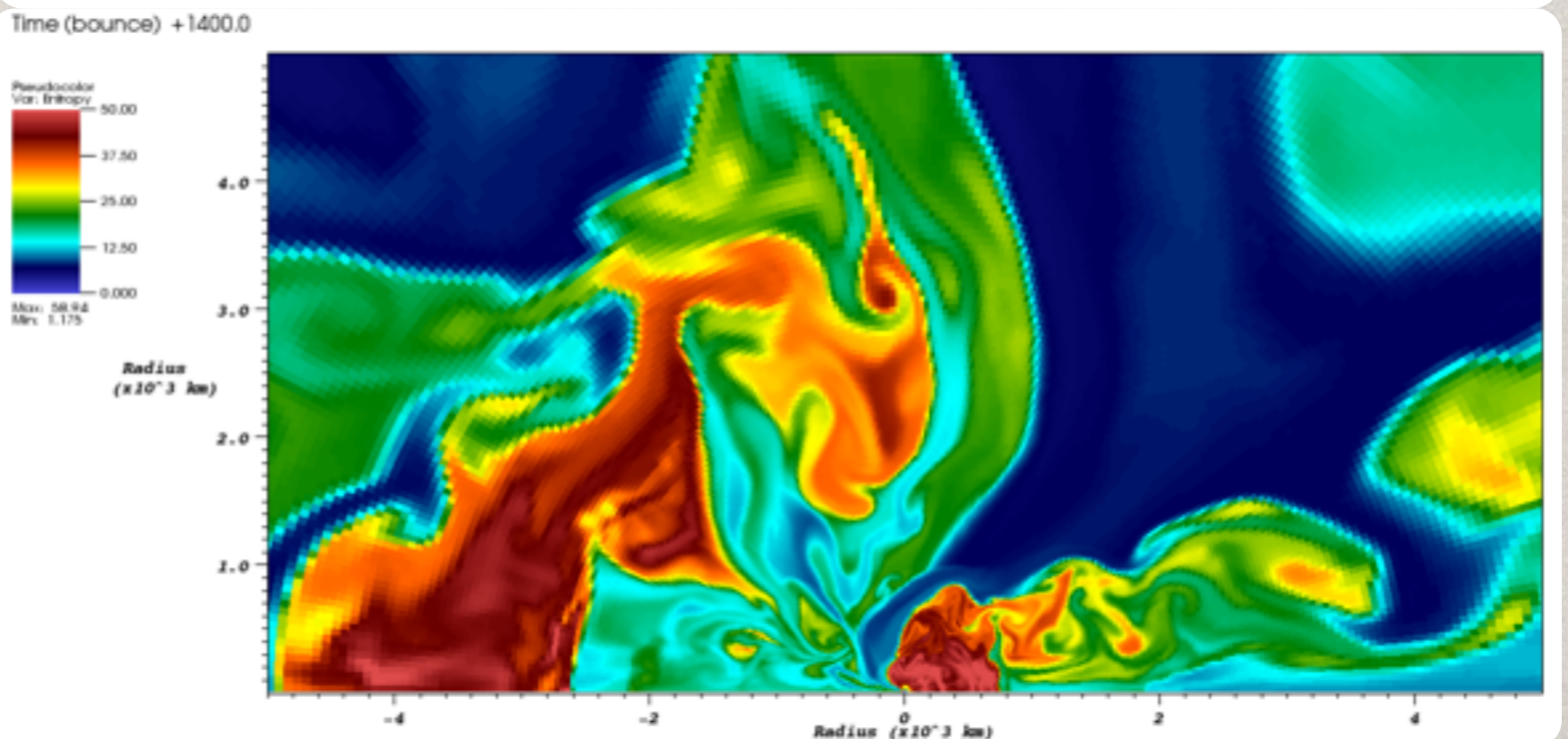
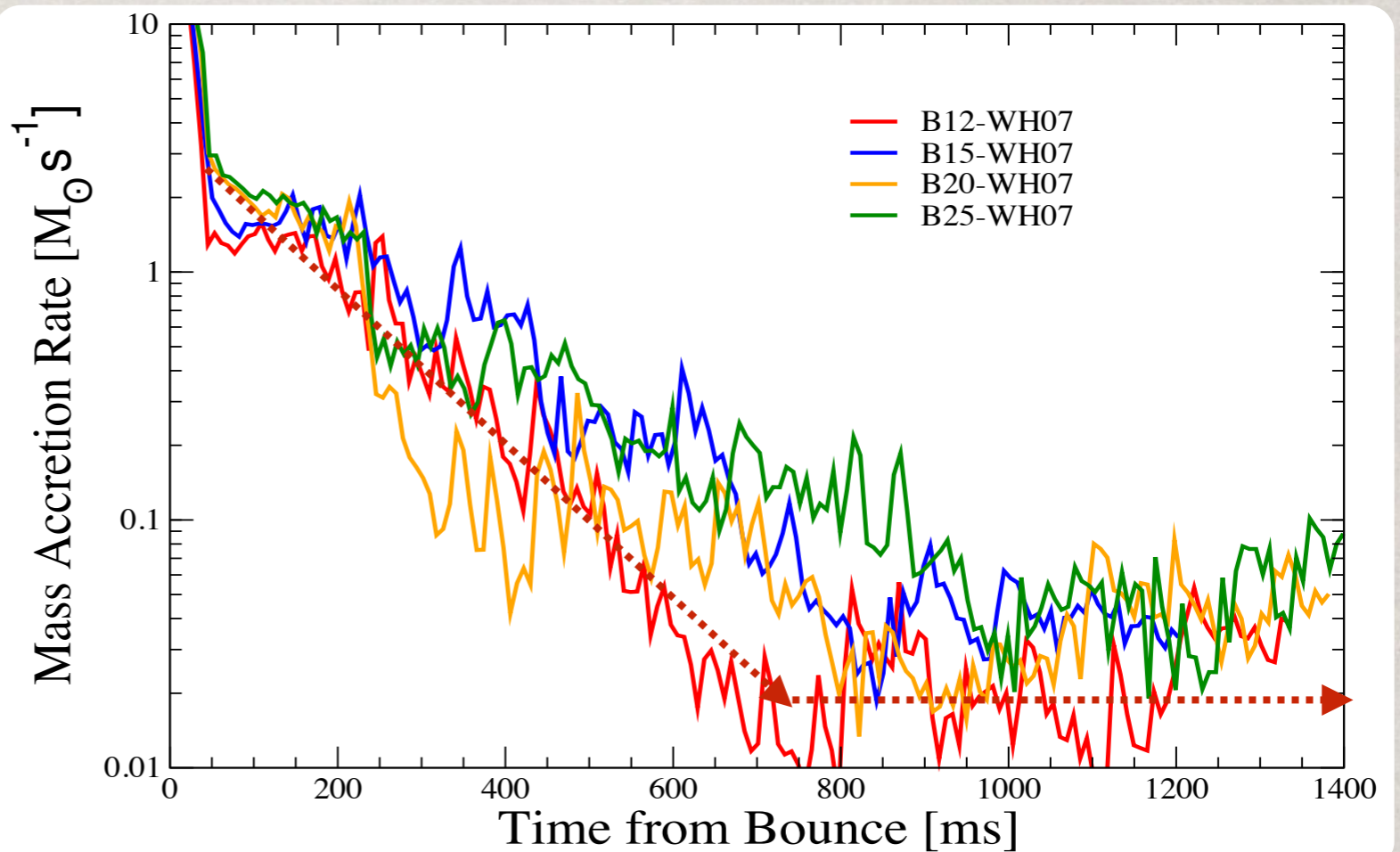


# END OF THE EXPLOSION?

Even in our most fully developed model, the explosion energy **has not leveled off** 1.3 seconds after bounce.

The reason is that **accretion continues** at an appreciable rate, showing no sign of abating.

This extends the “hot bubble” phase and **suppresses** the development of **the PNS wind**.

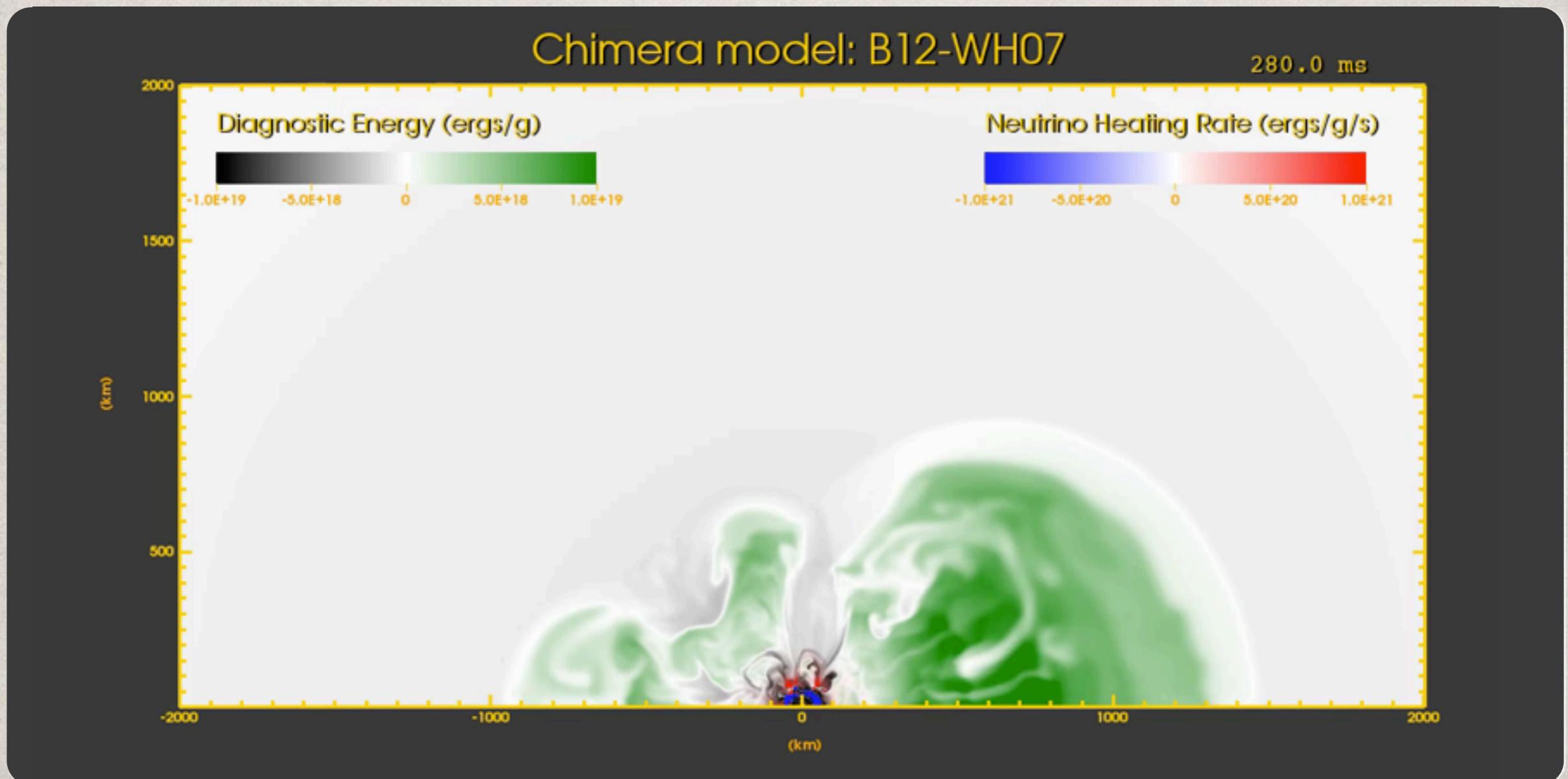




# THE PROBLEM OF FALLBACK

Some of the infalling matter at late times is making its **first approach** to the PNS, but much of the matter has been here before, having **expended energy** lifting the remainder of the star.

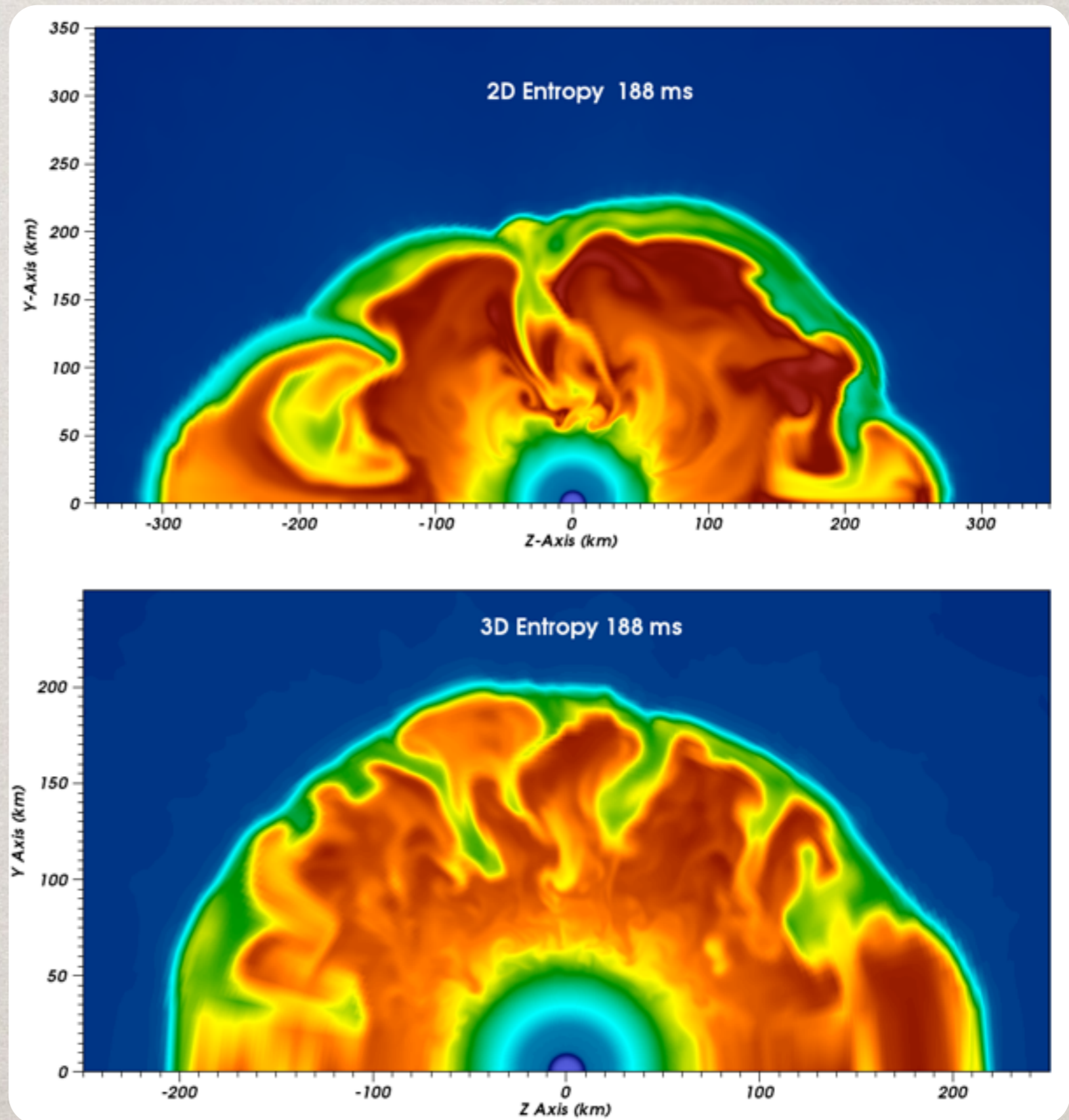
This continued accretion & heating impacts the **nucleosynthesis**.



# HOW DOES 3D COMPARE?

The vital question is “How well do 2D models follow the behavior of 3D?”

Thus far, we find that 3D models stay quasi-spherical longer and exhibit **longer delays** to the onset of explosion.

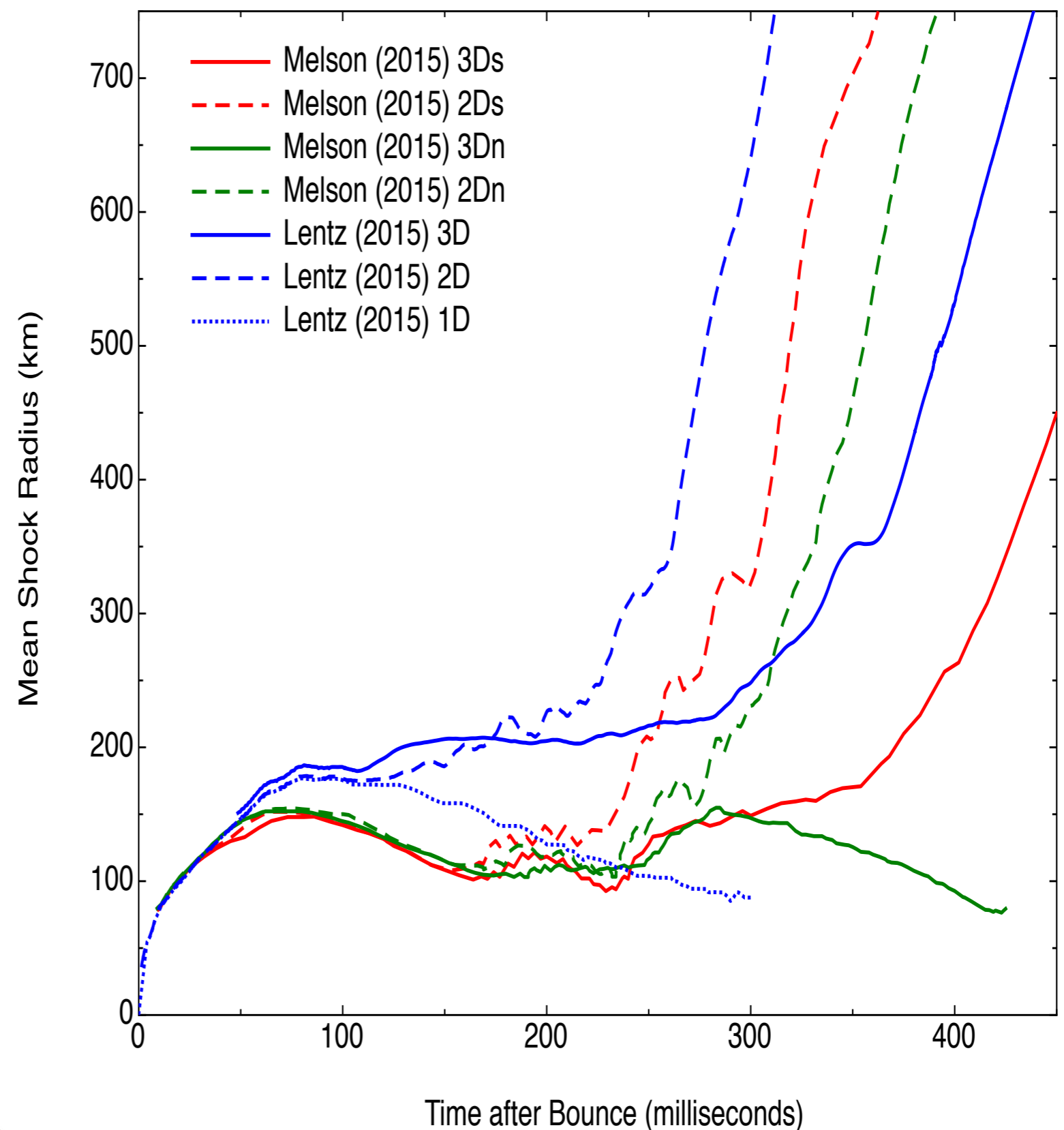


# HOW DOES 3D COMPARE?

The vital question is “How well do 2D models follow the behavior of 3D?”

Thus far, we find that 3D models stay quasi-spherical longer and exhibit **longer delays** to the onset of explosion.

This agrees with **self-consistent models** from Hanke et al (2013) and Melson et al (2015).

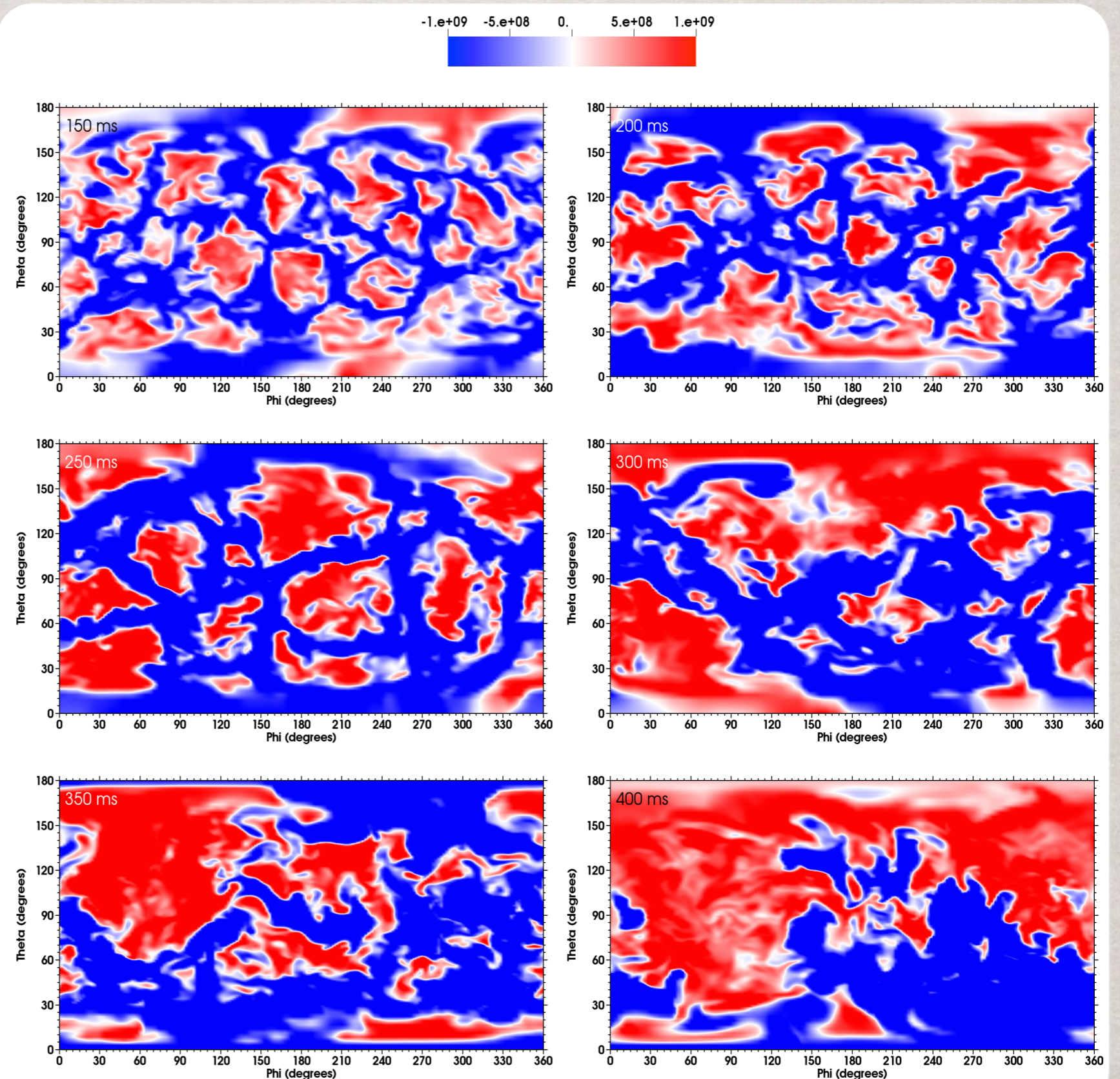


# GROWING PLUMES

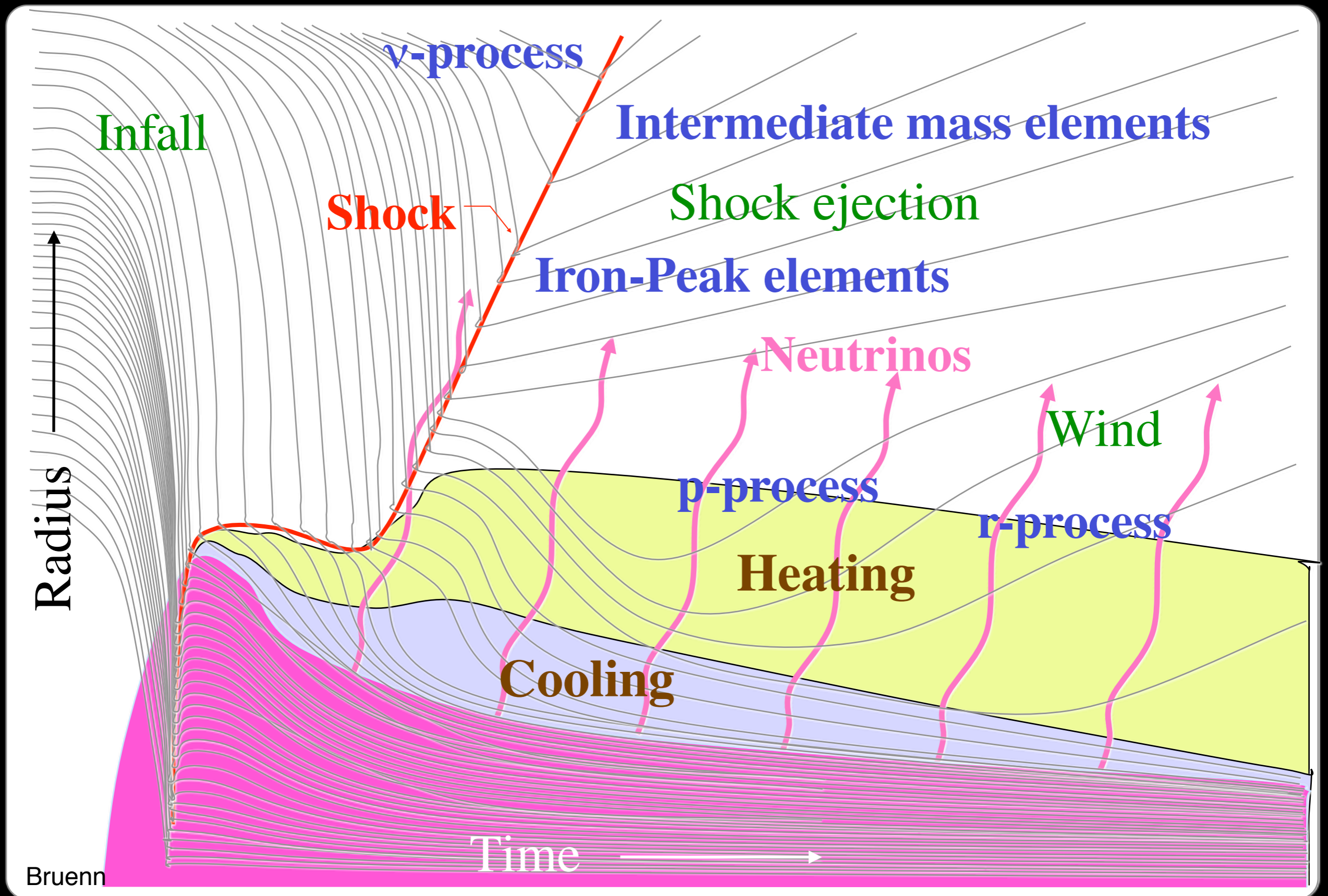
The explosion in 3D (as well as 2D) is preceded by the progress to fewer, larger plumes, see Fernandez (2015).

However, in 2D this progress is rapid.

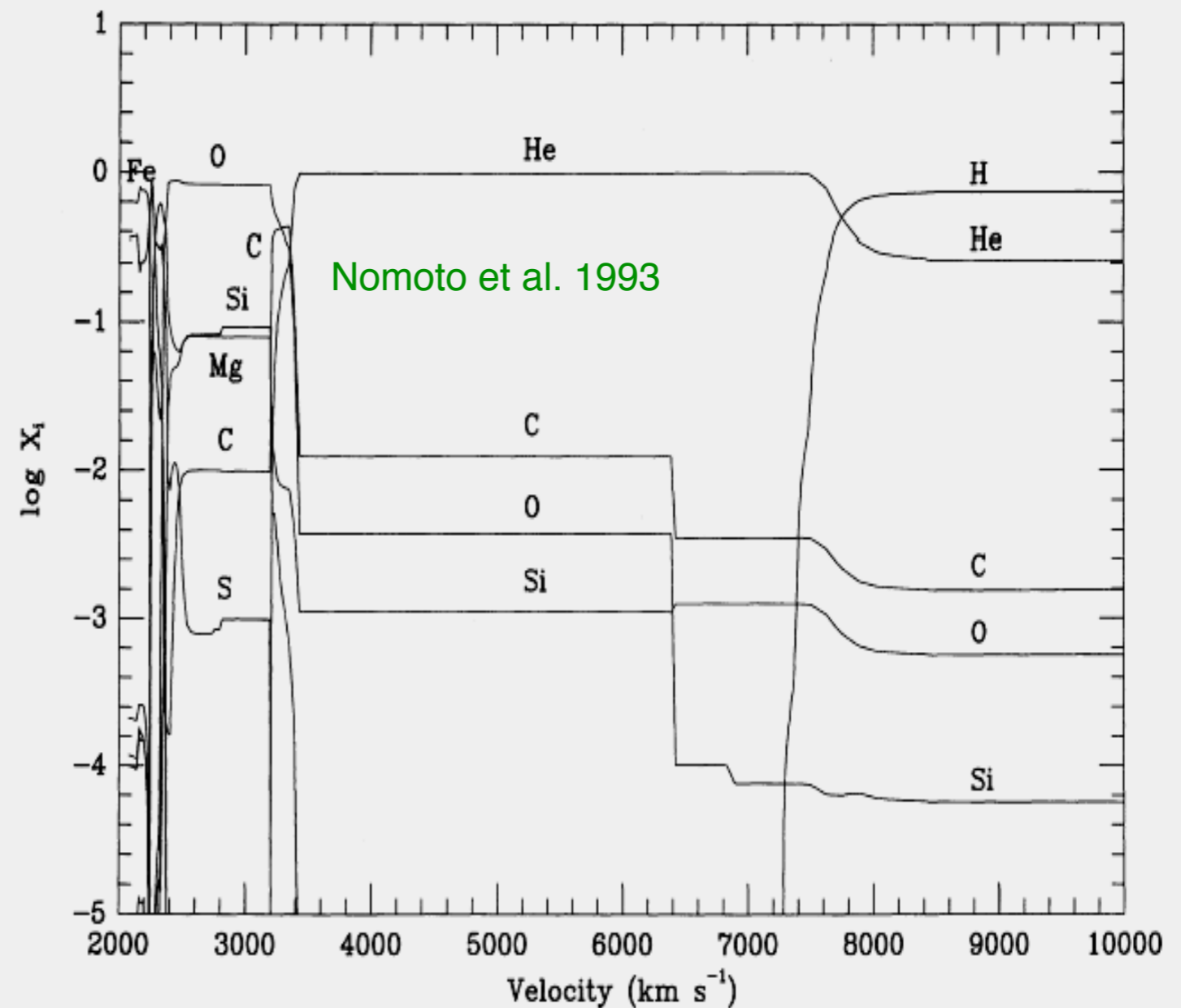
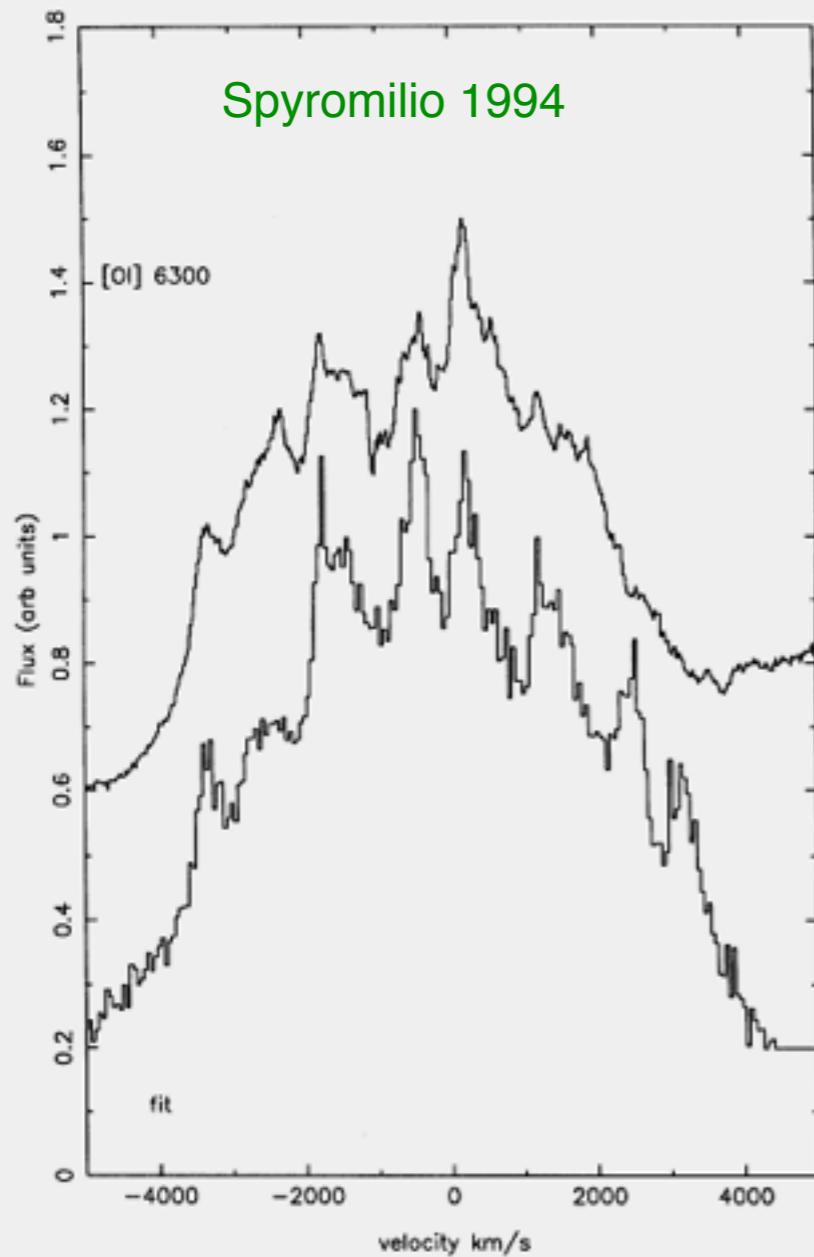
These larger plumes connect the shock to the **neutrinosphere**.



# SUPERNOVA NUCLEOSYNTHESIS



# TUNING THE EXPLOSION



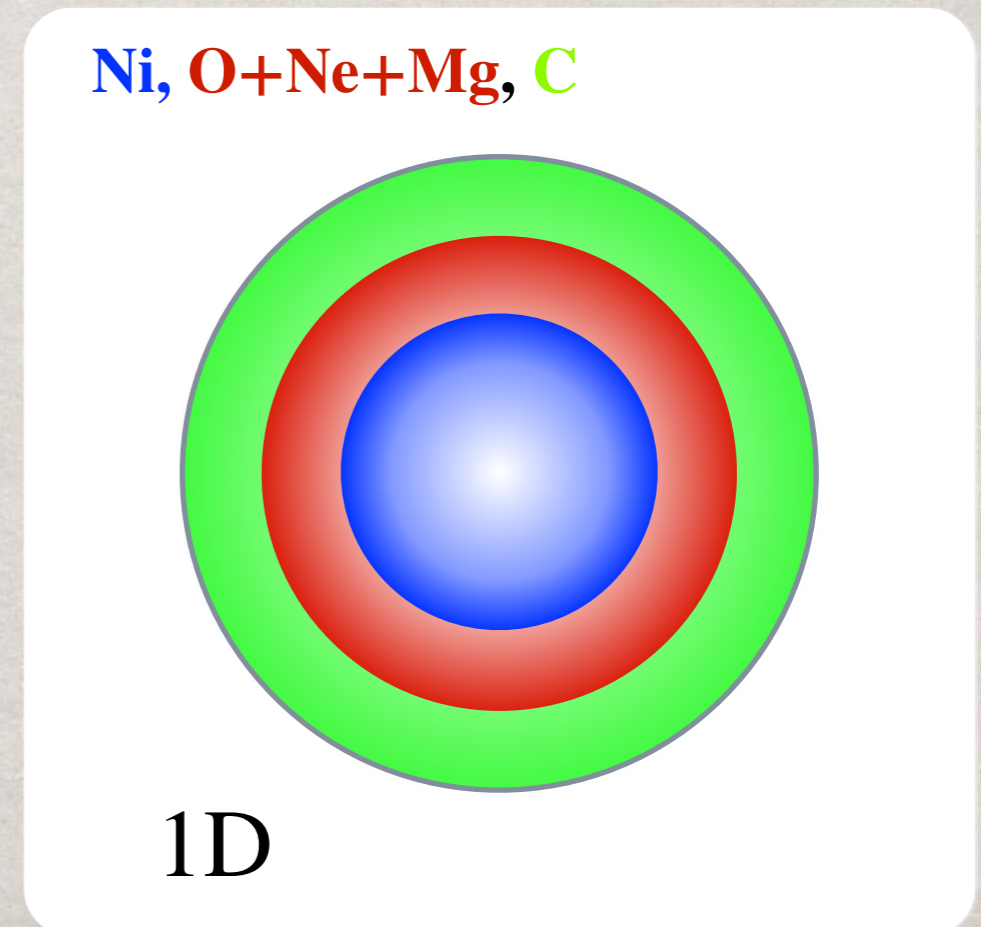
In parameterized nucleosynthesis models, 2 parameters, the **Bomb/Piston energy** and the **mass cut**, are constrained by observations of **explosion energy** and mass of  $^{56}\text{Ni}$  ejected.

# UNLEARN THE ONION

Observations tell us that the explosion, and the ejected elements, are **asymmetric**. Yet we rely on spherically symmetric models to understand supernova nucleosynthesis.



≠



# UNLEARN THE ONION

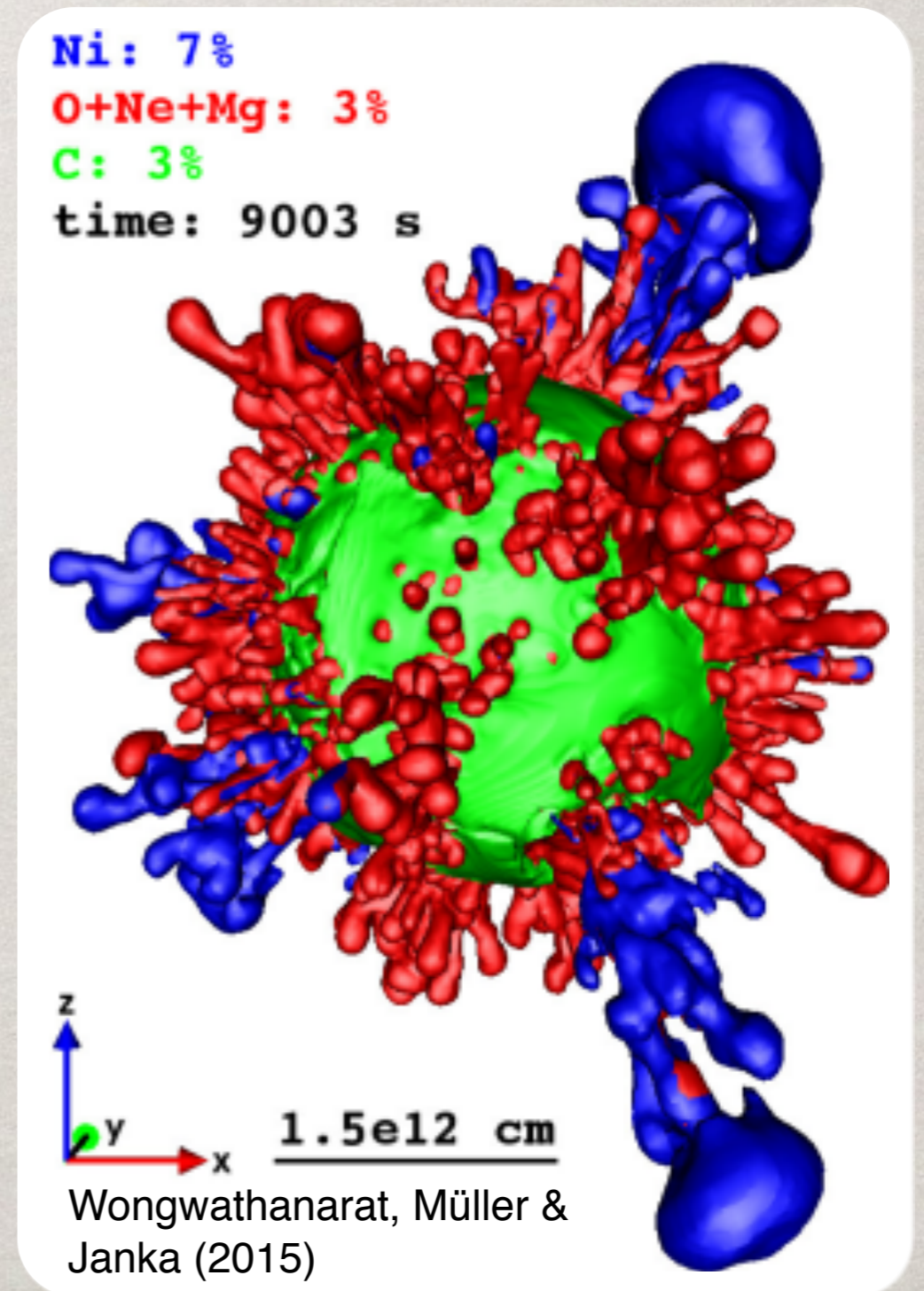
**Observations** tell us that the explosion, and the ejected elements, are **asymmetric**. Yet we rely on spherically symmetric models to understand supernova nucleosynthesis.

This colors our discussion, for example the notion that the **matter created closest to the neutron star** is most sensitive to the “**mass cut**”.



?

≡

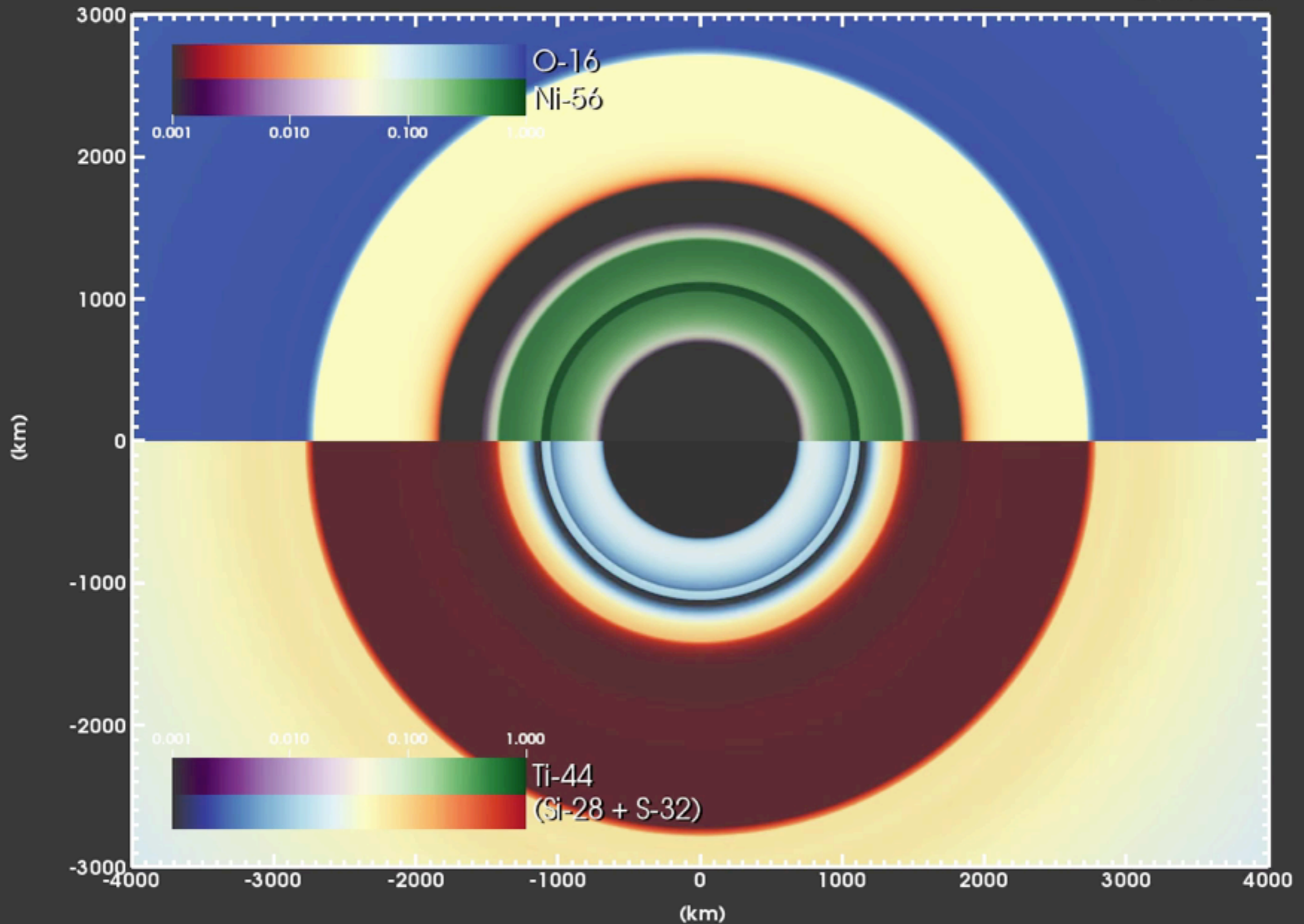




# NUCLEOSYNTHESIS: THE MOVIE

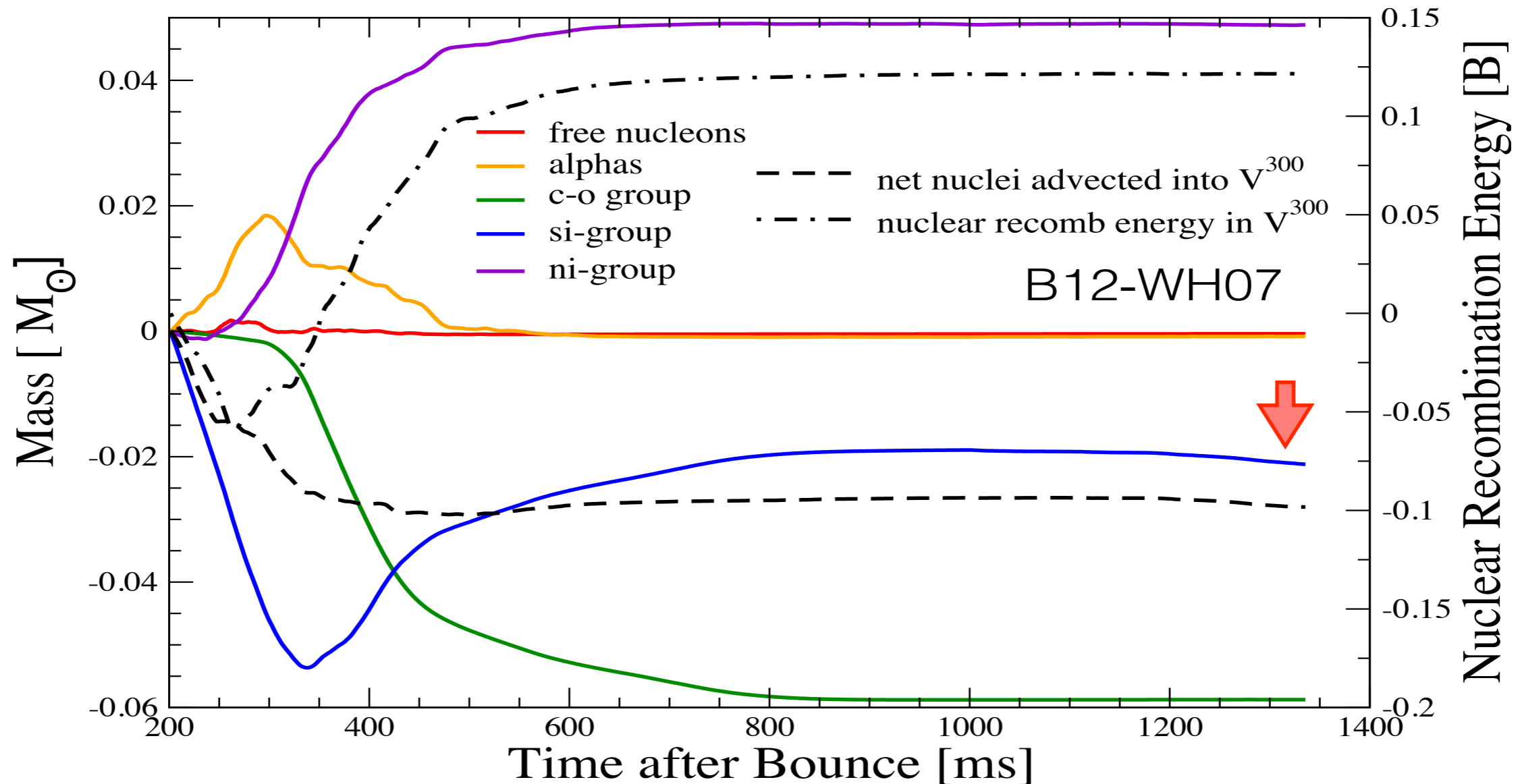
Chimera model: B12-WH07

-258.2 ms



# FINISHED COOKING?

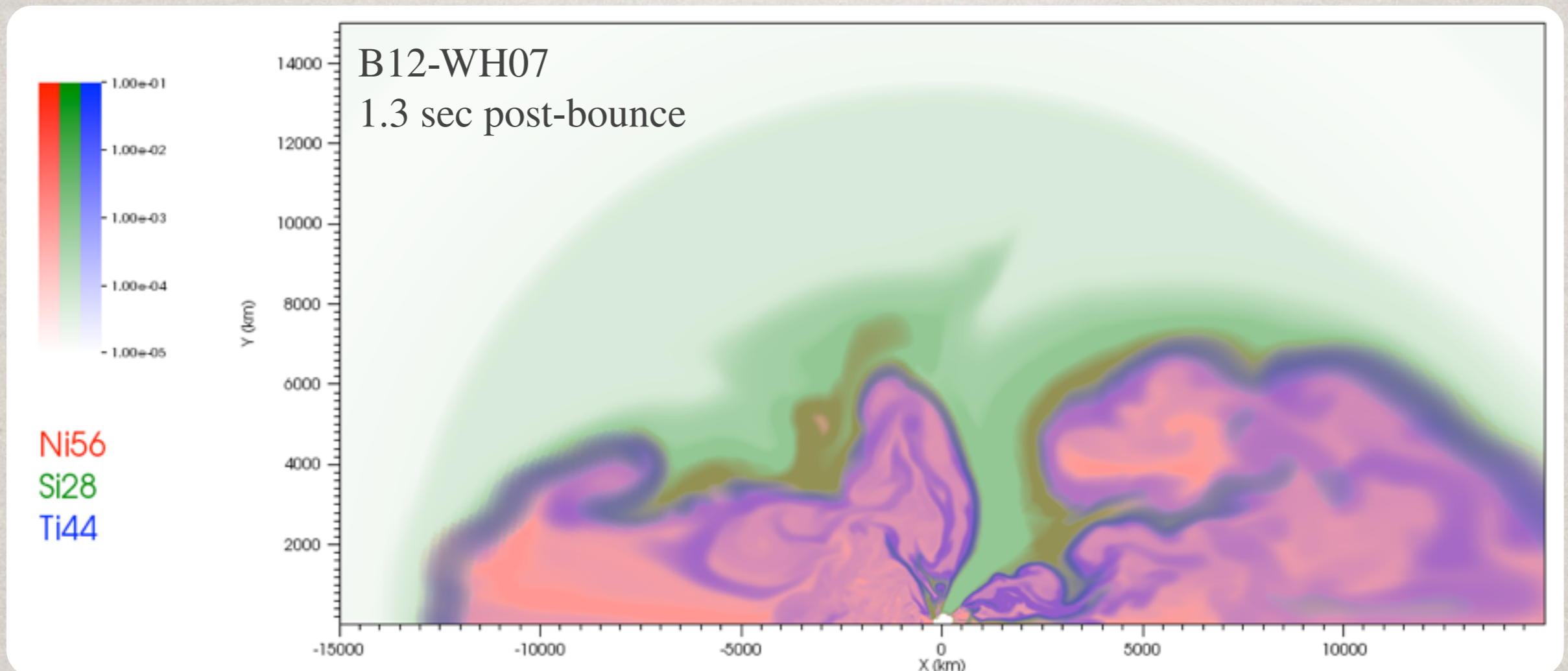
By 800–900 ms after bounce, **shock burning** in the  $12 M_{\odot}$  model is **nearly complete** with shock temperature  $\sim 2$  GK.



Matter continues to **fall inward** of 300 km beyond one second, predominantly from cut-off down flows.

# NUCLEOSYNTHESIS LIMITS

We can calculate nucleosynthesis directly with the  $\alpha$ -network (plus neutrons, protons and auxiliary heavy) in CHIMERA.



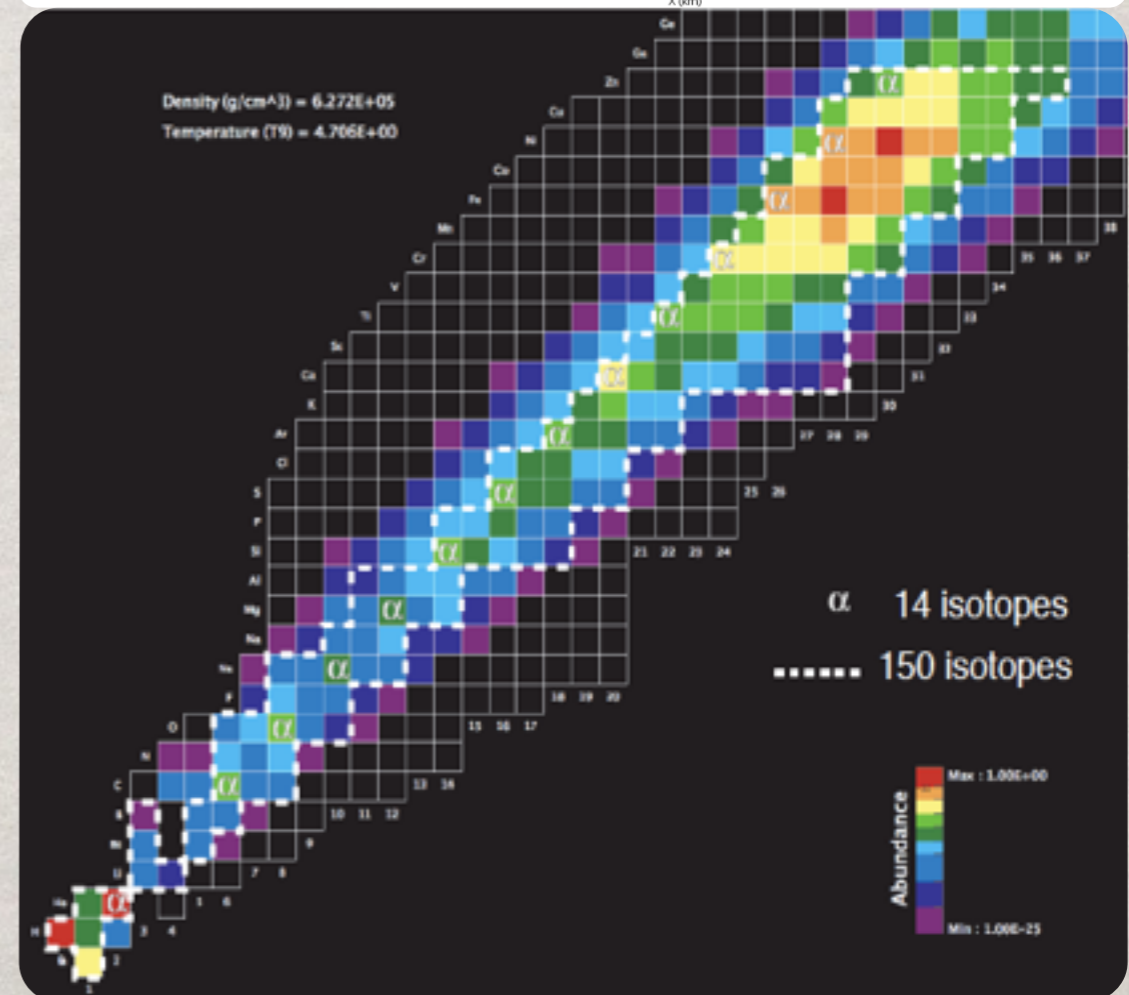
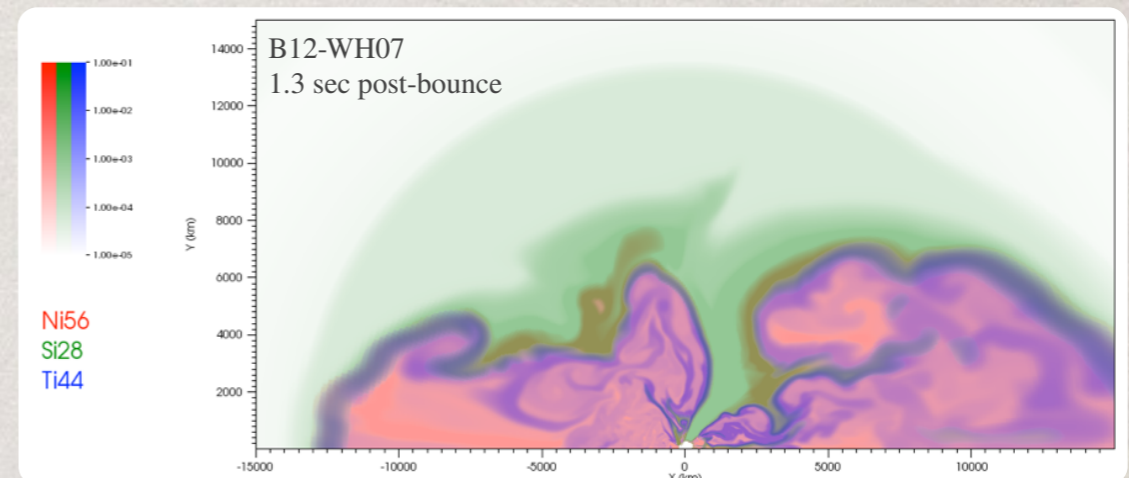
# NUCLEOSYNTHESIS LIMITS

We can calculate nucleosynthesis directly with the  $\alpha$ -network (plus neutrons, protons and auxiliary heavy) in CHIMERA.

As the mass cut resolves, we can examine the nucleosynthesis with **increasing accuracy**.

But parameterized models consider **hundreds** (or even thousands) of **species** within the supernova simulation.

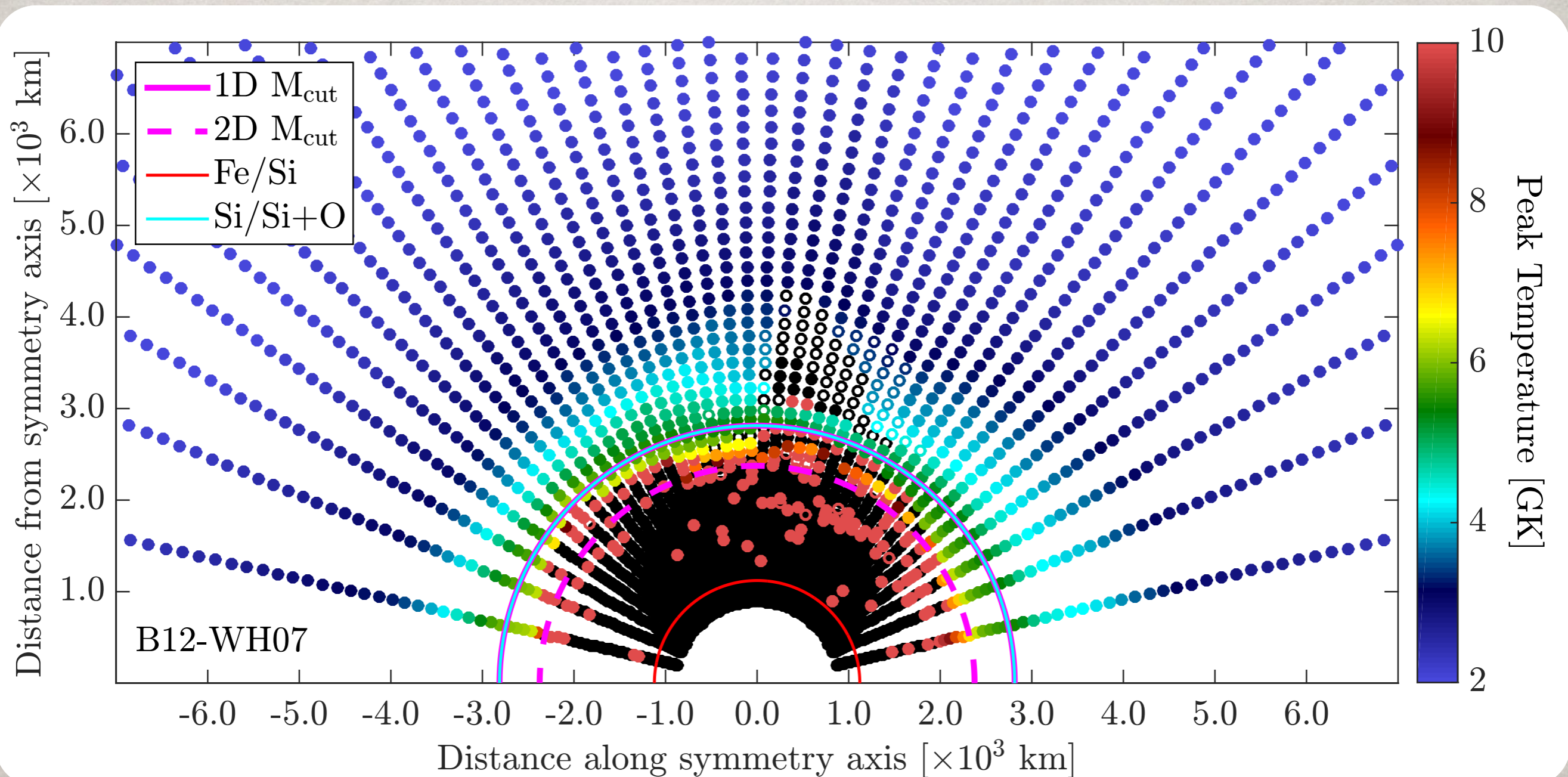
Doing the same in CHIMERA requires post-processing of Lagrangian tracer particles, or using a **larger network** within the supernova models.



# TRACING THE MASS CUT

Post-processing of **tracer particles** is required for nucleosynthesis predictions beyond the built-in network,  $\alpha$ -network or otherwise.

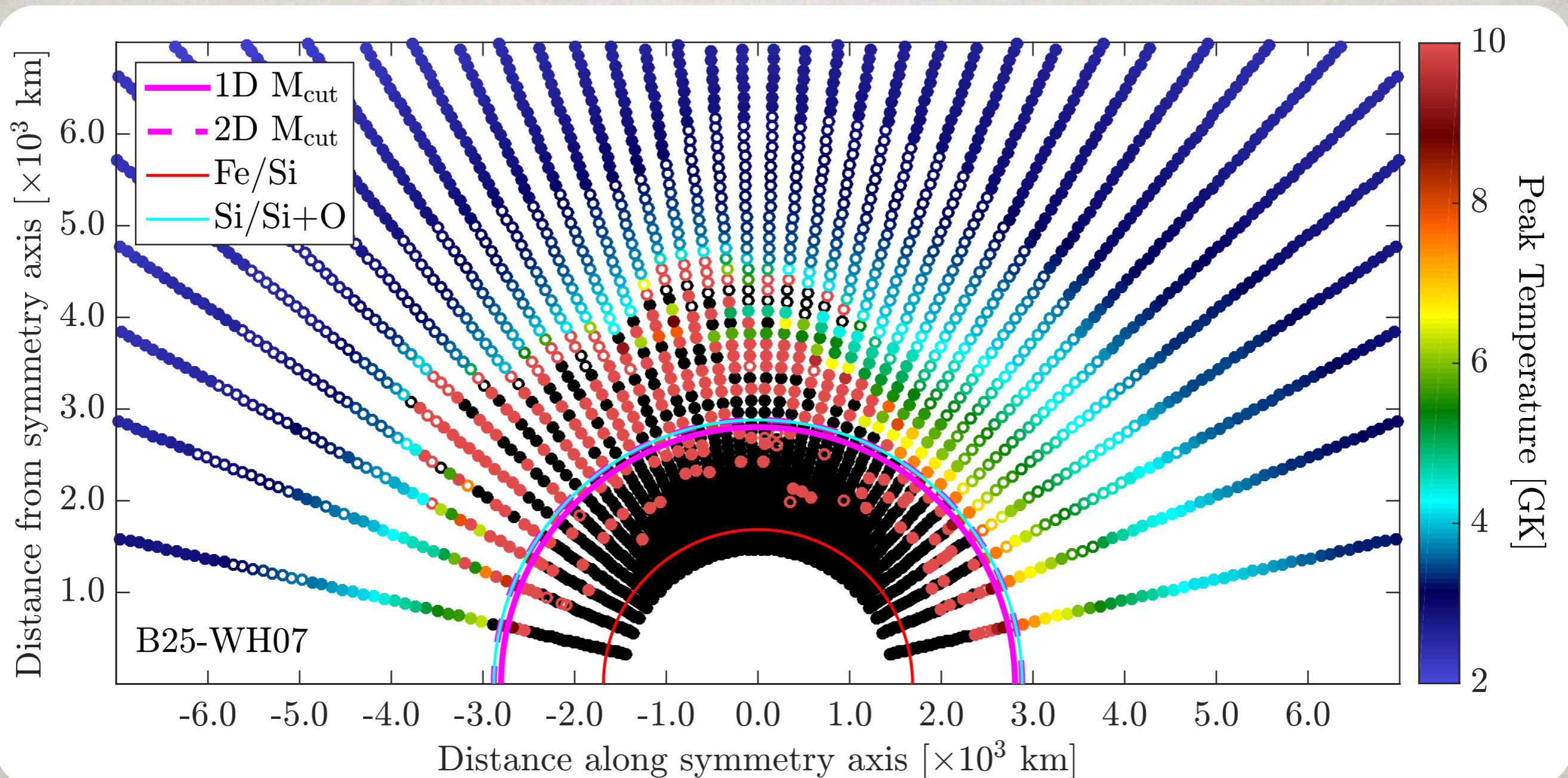
Their Lagrangian view also reveals the complexity of the **mass cut**.



# TRACING THE MASS CUT

Post-processing of **tracer particles** is required for nucleosynthesis predictions beyond the built-in network,  $\alpha$ -network or otherwise.

Their Lagrangian view also reveals the complexity of the **mass cut**.

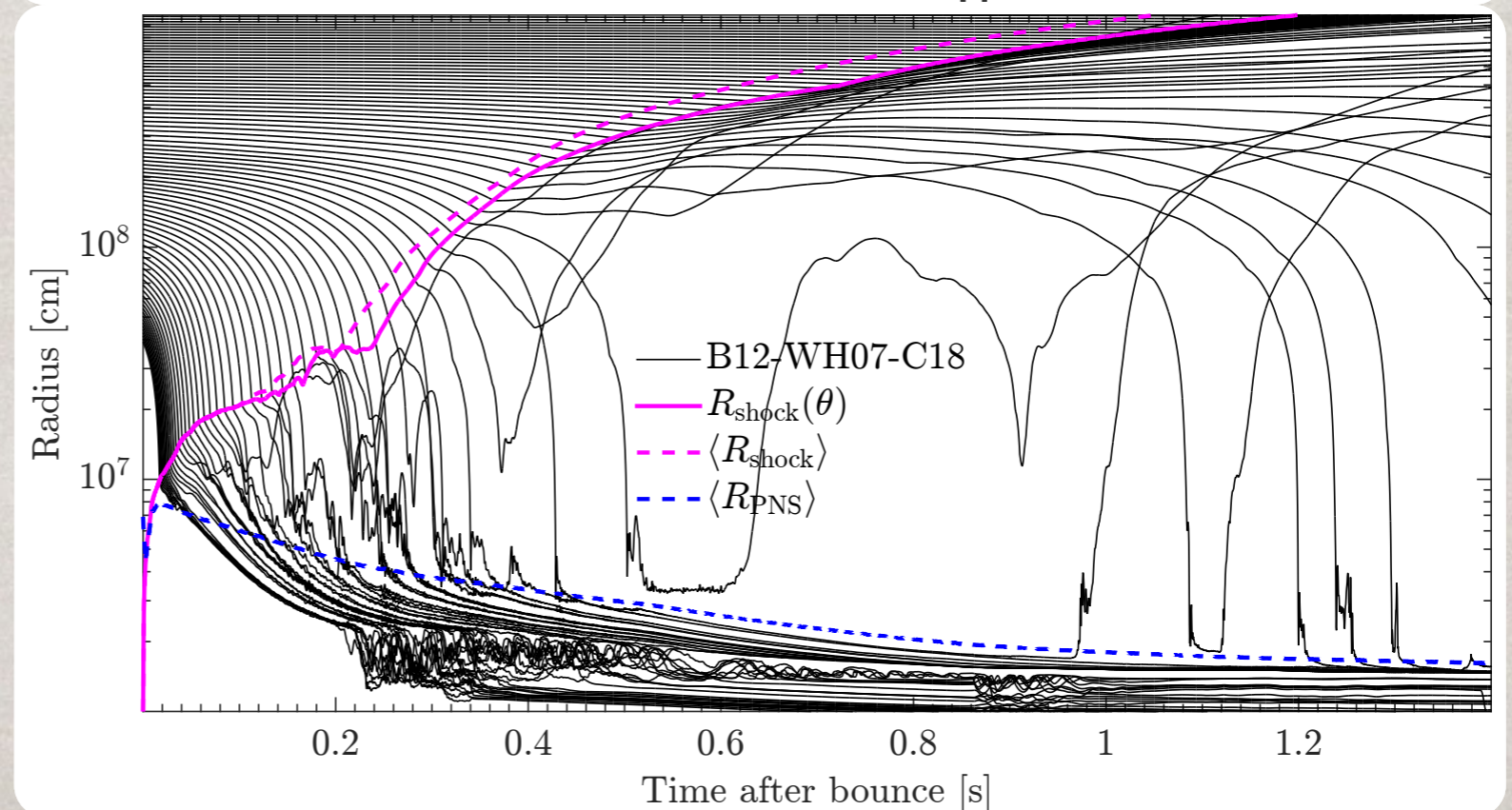
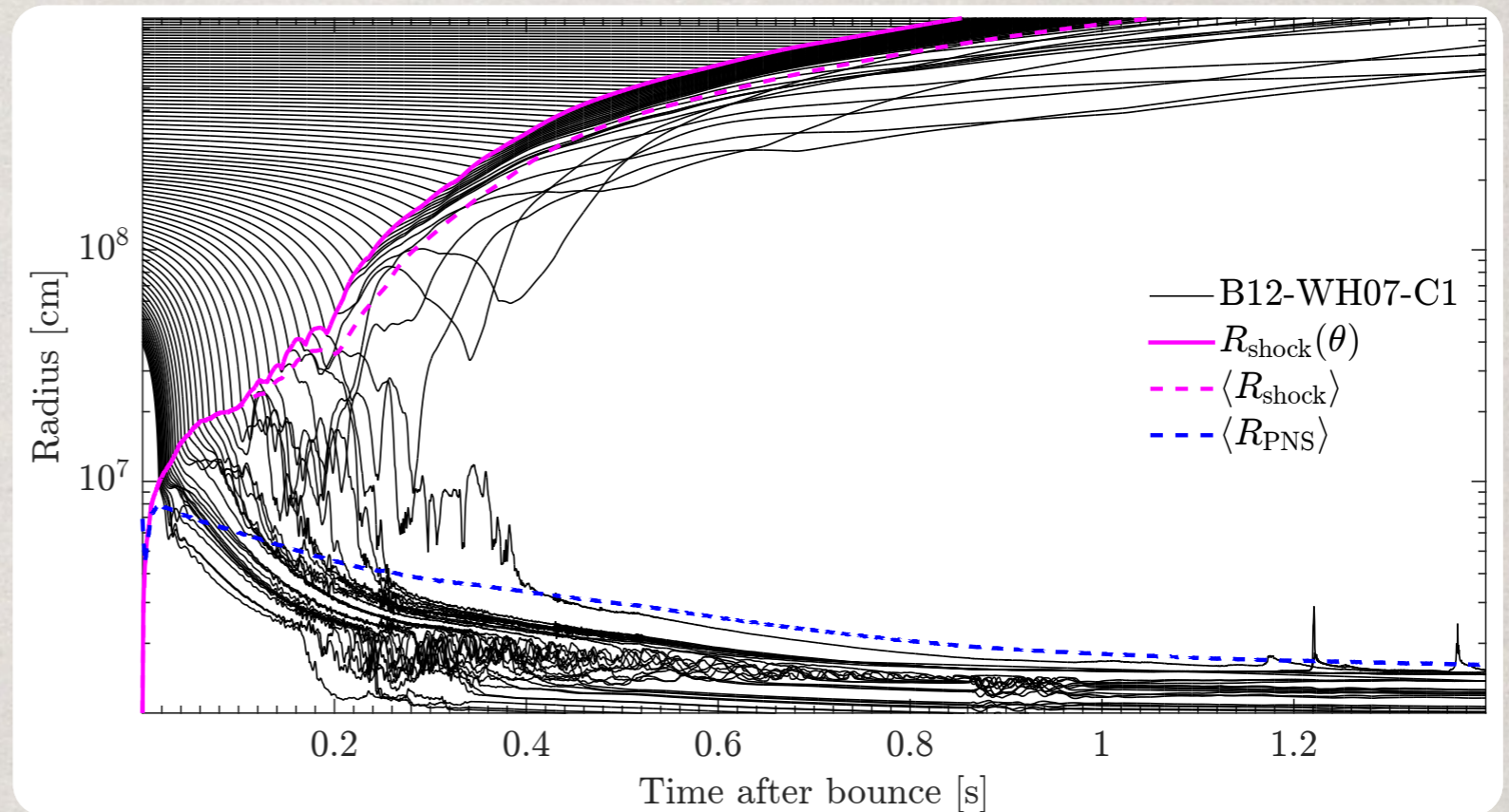


# LATITUDE DEPENDENCE

With 40 columns of tracers in each model, we can examine the fate of the star as a function of latitude.

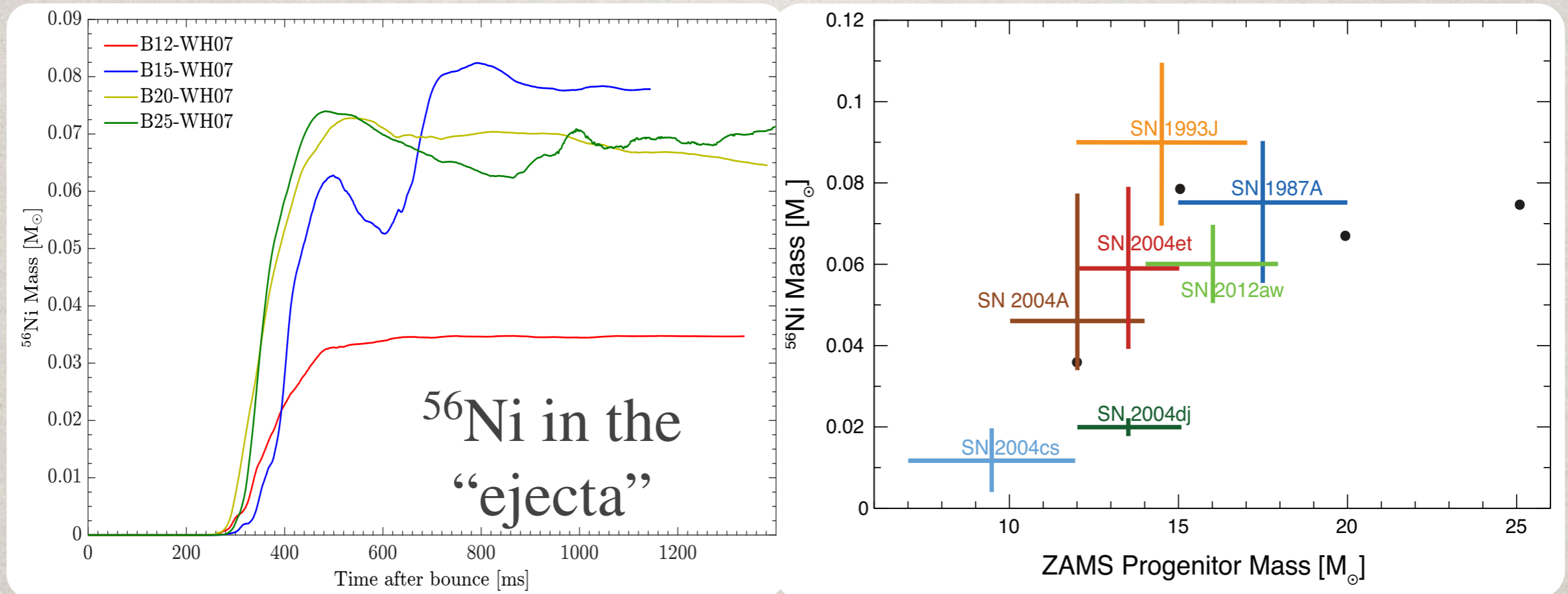
Near the pole, separation between ejecta and PNS develops rapidly and robustly.

Matter from near the equator continues to accrete and be ejected through the end of the simulations.



# NICKEL MASS

Beyond the explosion energy, perhaps the most important observable is the mass of  $^{56}\text{Ni}$ , because of its relation to the light curve.



The ejected  $^{56}\text{Ni}$  mass **saturates in time** with the explosion energy.

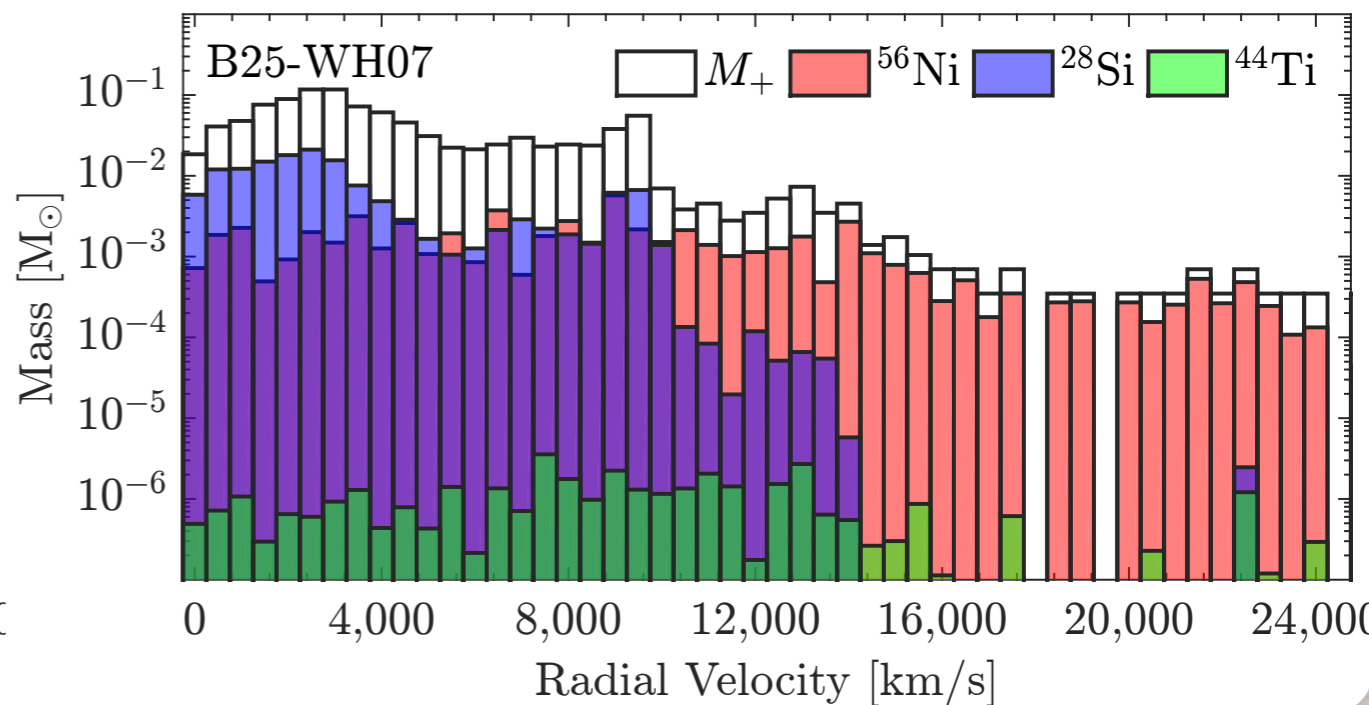
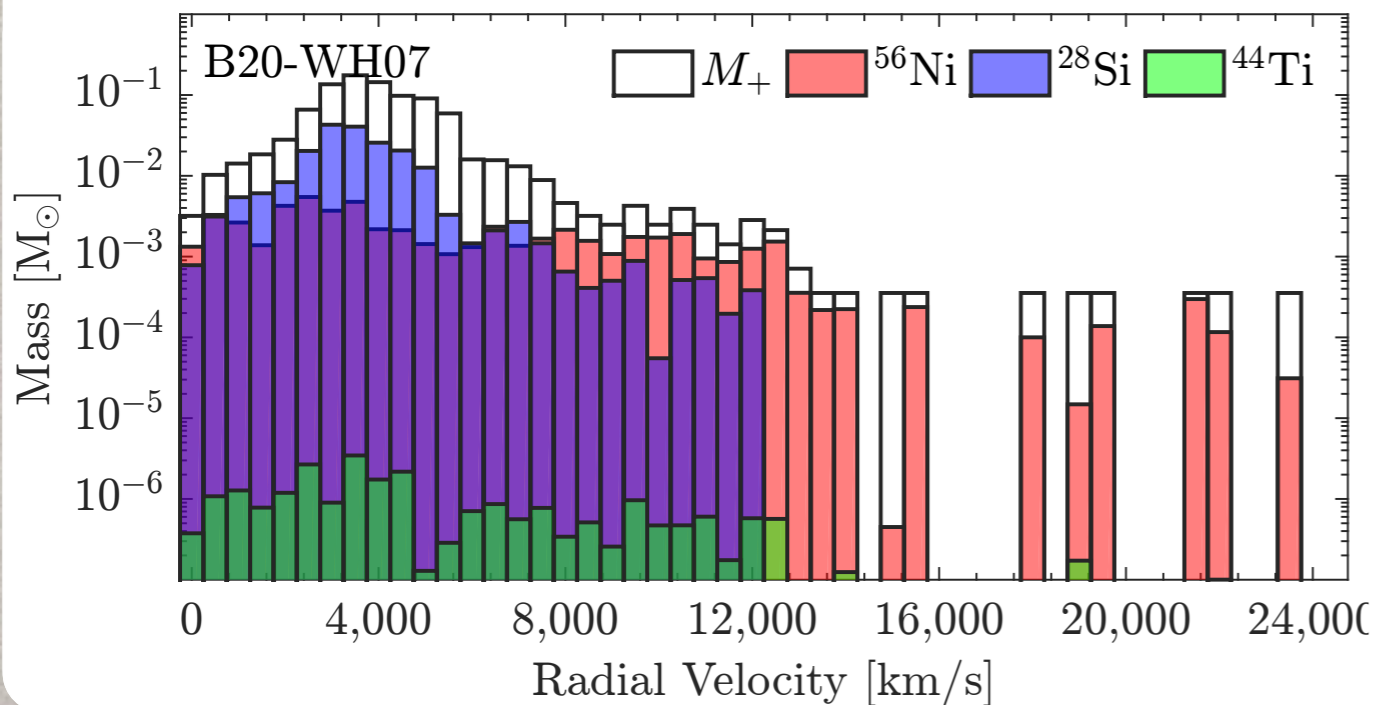
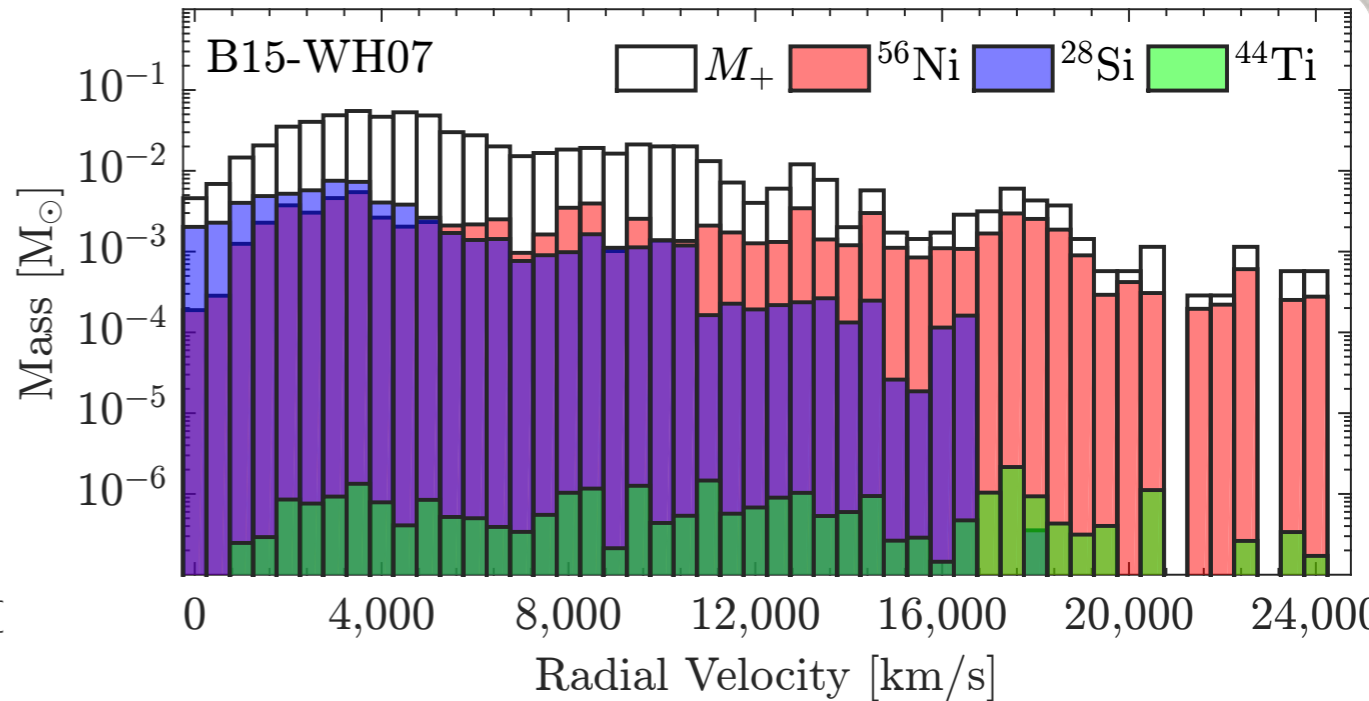
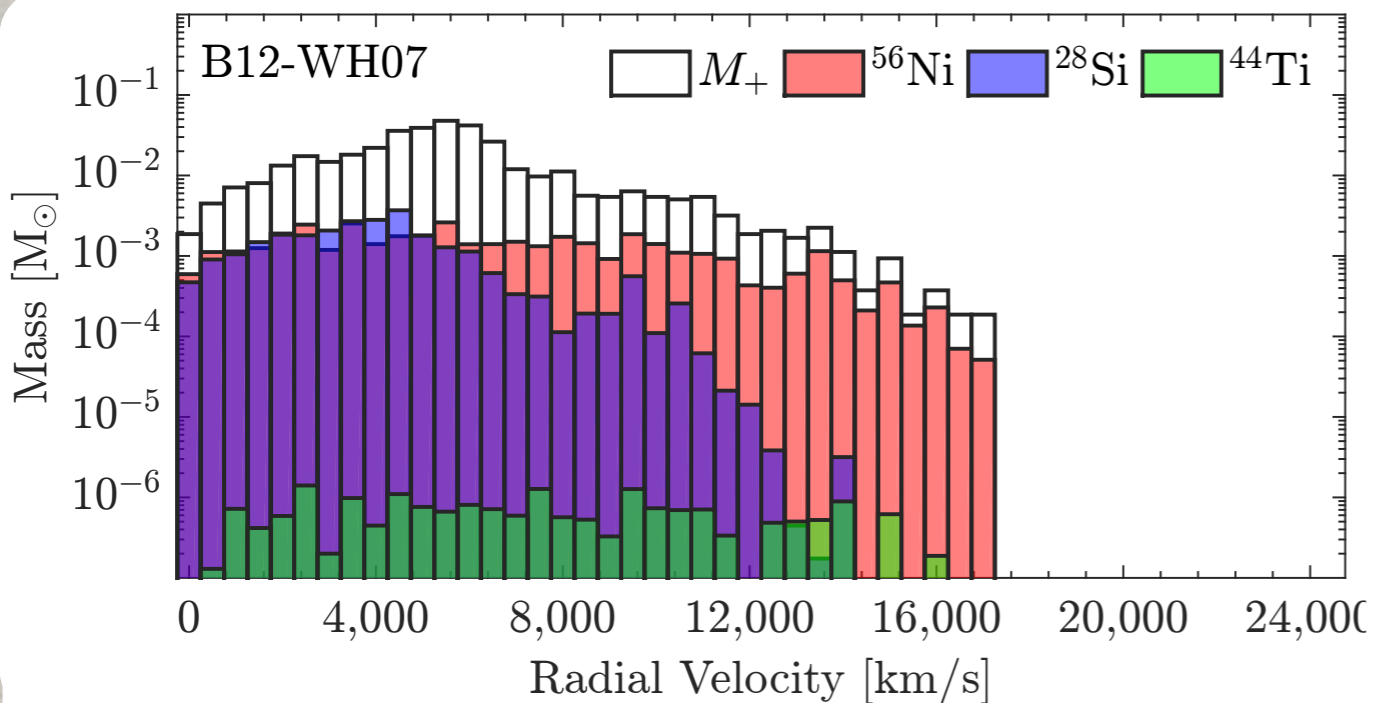
Results are reasonable, when compared to **observations**.

**Fallback over longer timescales is uncertain.** Recent studies are finding differing results on fallback and  $^{56}\text{Ni}$  has higher velocity.



# VELOCITY DISTRIBUTION

Unlike 1D, **Nickel** and **Titanium** have higher velocities than **Silicon** and **Oxygen**, thus they are not preferentially sensitive to fallback.

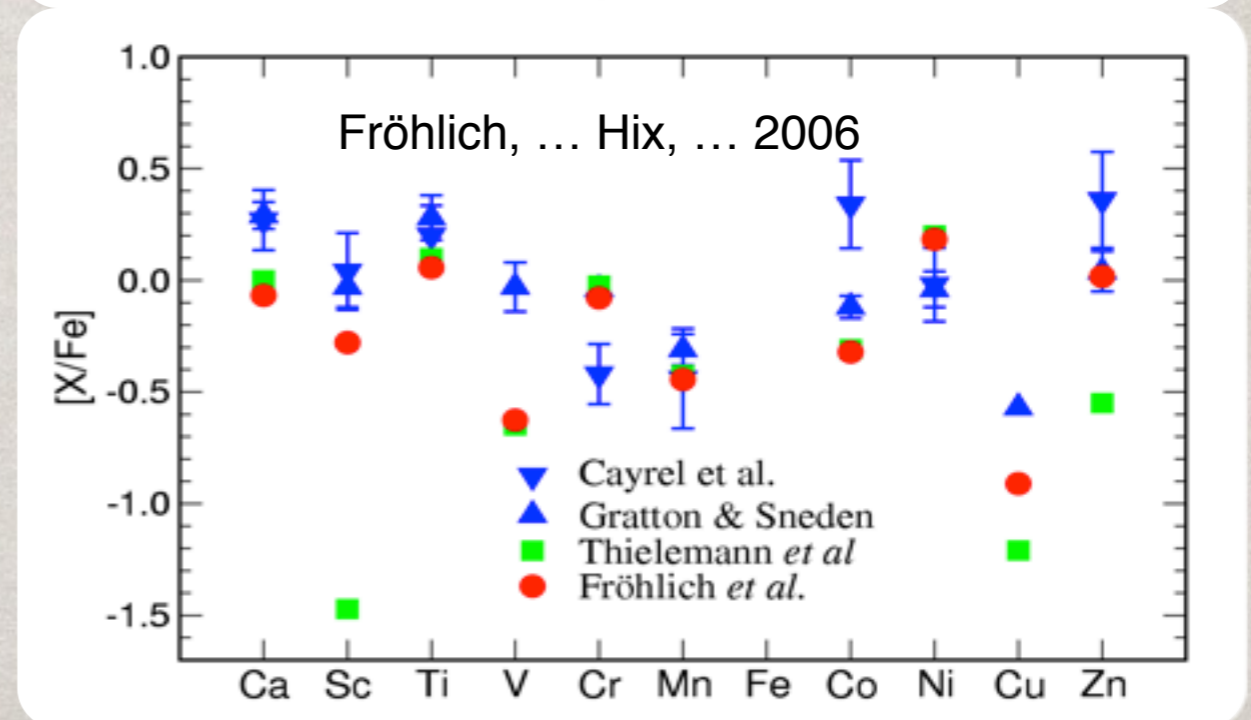
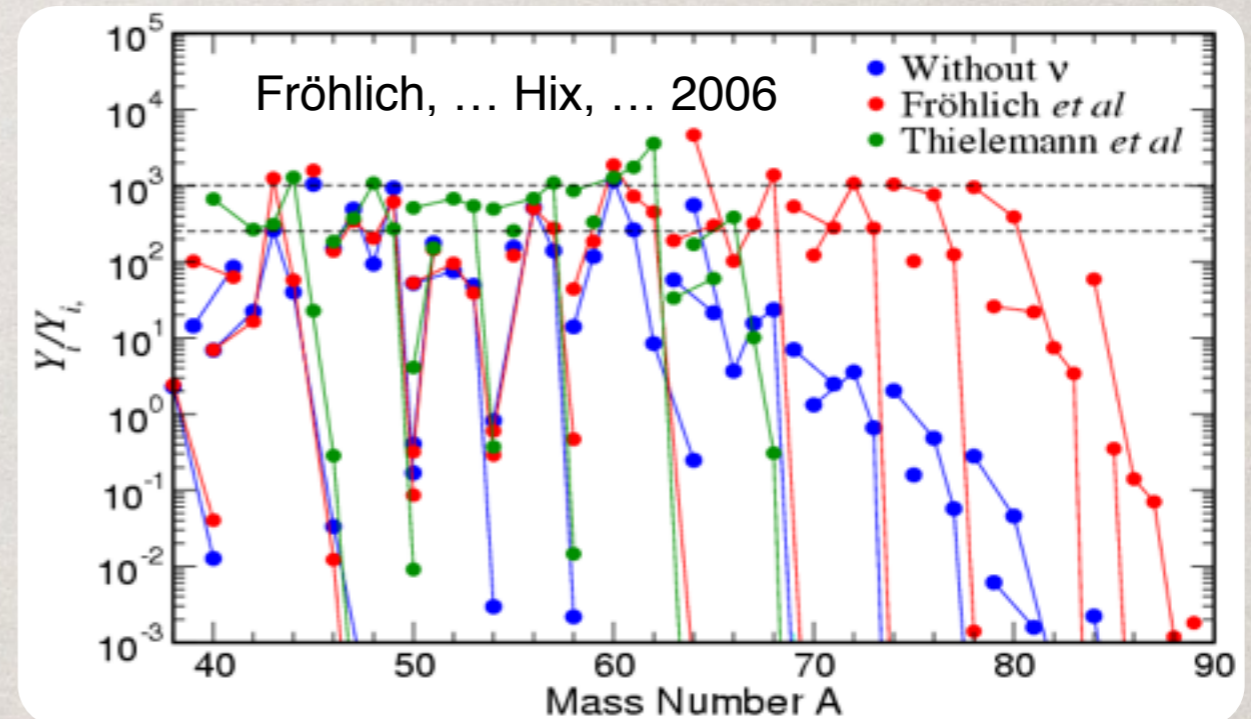


# NEUTRINOS & NUCLEOSYNTHESIS

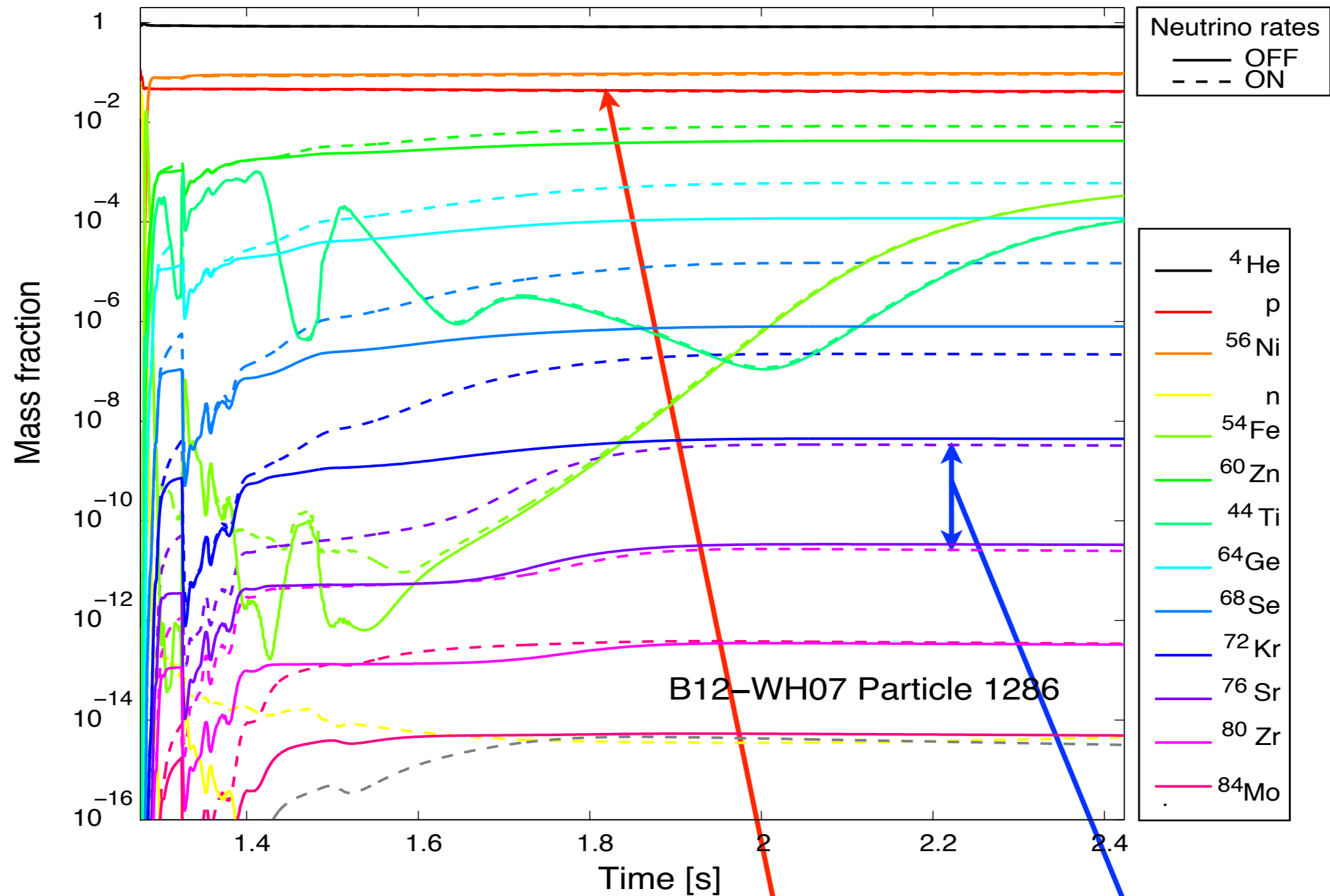
Despite the perceived importance of neutrinos to the core collapse mechanism, models of the nucleosynthesis have largely ignored this important effect.

Nucleosynthesis from  $\nu$ -powered supernova models shows several notable improvements.

1. Over production of **neutron-rich iron and nickel reduced**.
2. Elemental abundances of **Sc, Cu & Zn** closer to those **observed** in metal-poor stars.
3. Potential source of **light p-process nuclei** ( $^{76}\text{Se}$ ,  $^{80}\text{Kr}$ ,  $^{84}\text{Sr}$ ,  $^{92,94}\text{Mo}$ ,  $^{96,98}\text{Ru}$ ).



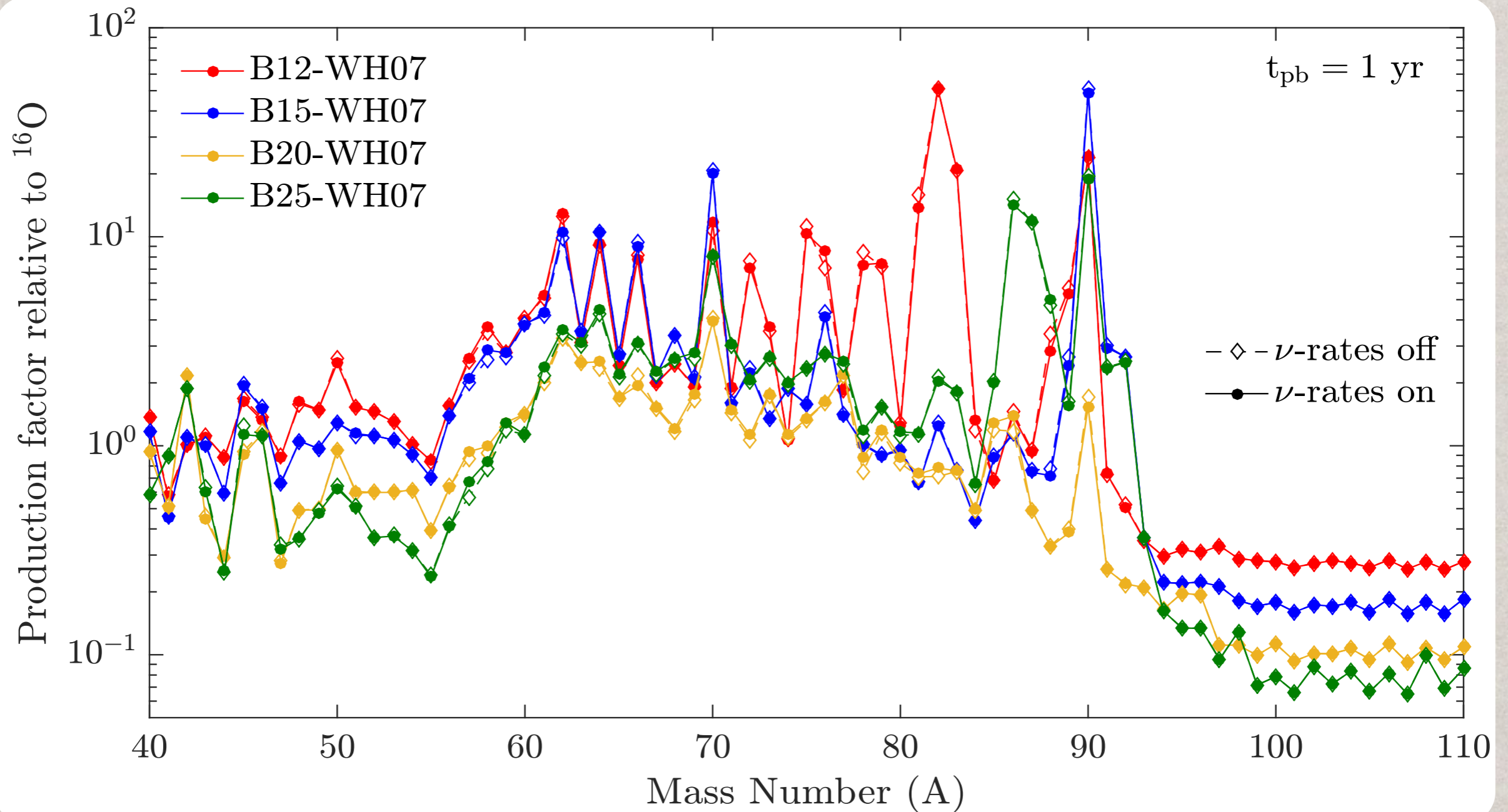
# $\nu$ P-PROCESS ...



Our preliminary results show **proton-rich ejecta**, but the  $\nu$ p-process (dotted lines) occurs for only a handful of particles.

# ... IS MISSING

The  $\nu p$ -process is very weak in these models.



The suppression of the PNS wind is delaying or preventing a strong  $\nu p$ -process from occurring.

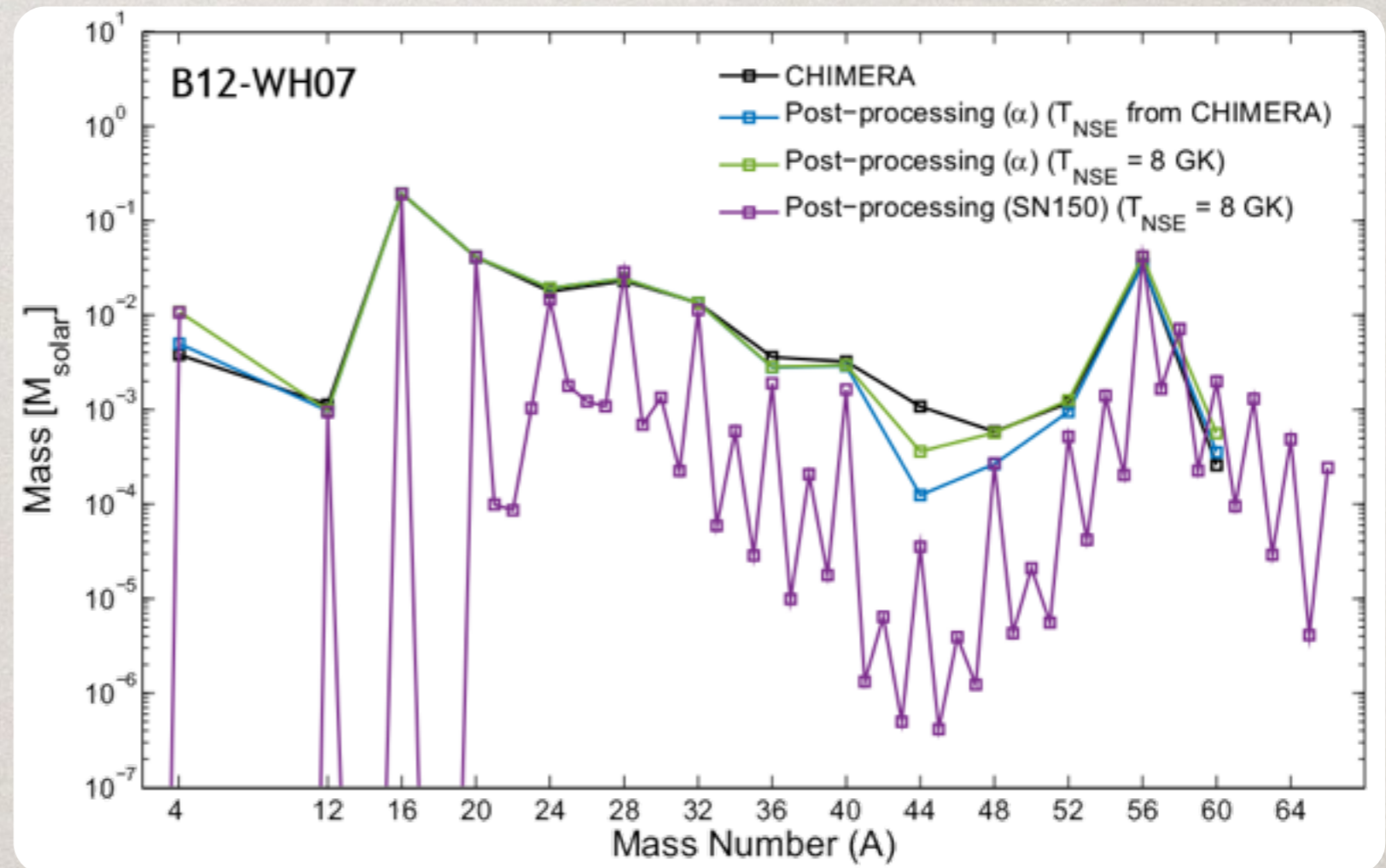
# NUCLEOSYNTHESIS TESTING

By computing the post-process nucleosynthesis in the **same fashion** as that built into CHIMERA, we learn about the limits of the tracers.

Products of  $\alpha$ -rich freezeout are **poorly captured** by the post-processing.

Accurately capturing the  $\alpha$ -rich freezeout also requires **transitioning out of NSE** at temperatures  $> 6$  GK.

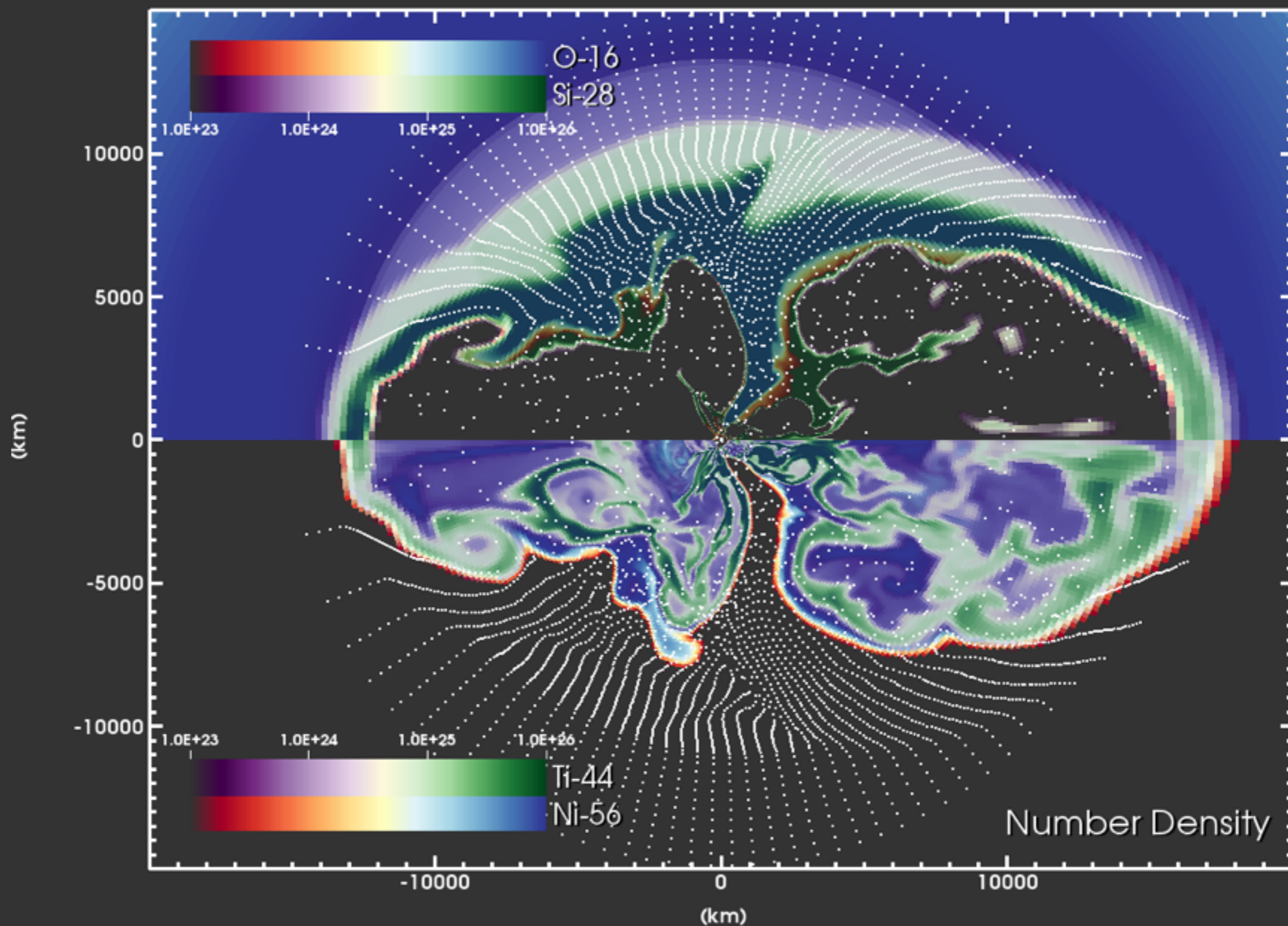
The limitations of the  $\alpha$ -network, when compared to a **more realistic network**, are most evident in the  $\alpha$ -rich freezeout and for  $A > 56$ .



# TRACKING LOW DENSITY

Chimera model: B12-WH07

1336.0 ms



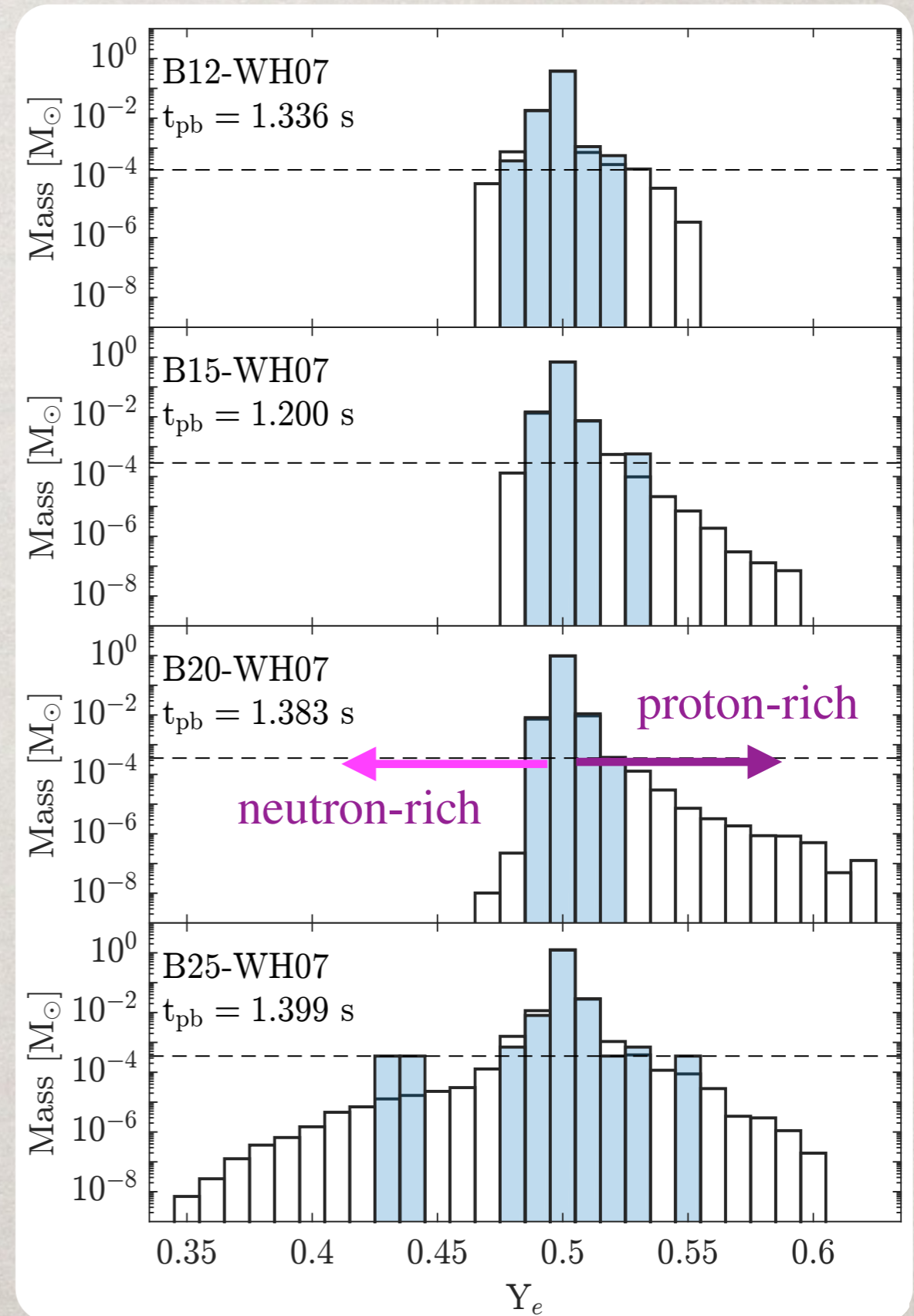
# TRACER RESOLUTION

Another view of the limitations of the tracer resolution is the **distribution in the electron fraction** of the ejecta.

Tracer resolution clearly **limits the production of more exotic species.**

For the **B-series**, run to 1.2-1.4 s after bounce, **this is the largest uncertainty**, though it only affects  $\alpha$ -rich freezeout.

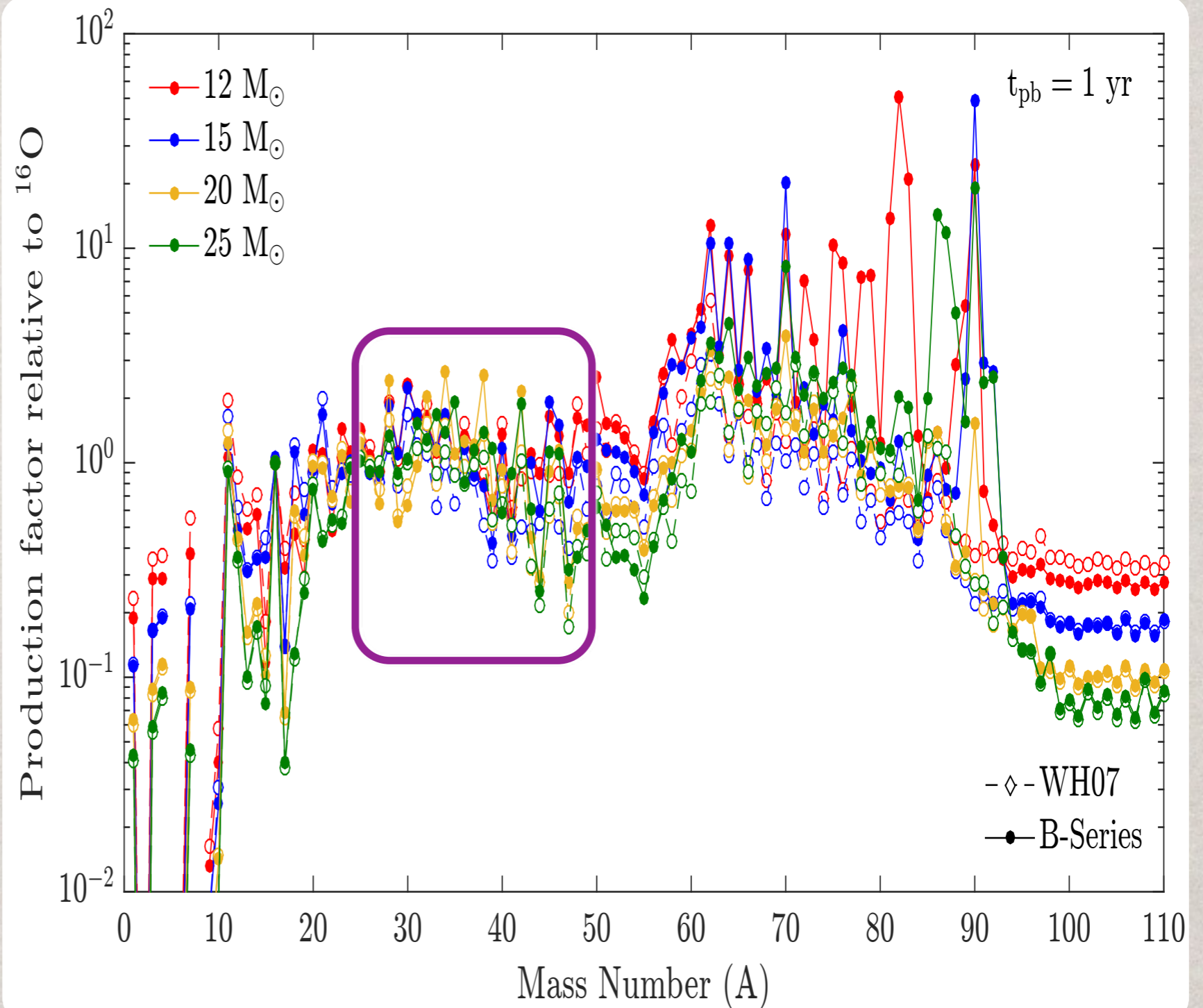
Model	Particles	$M_{\text{tracer}} [M_{\odot}]$
B12-WH07	4000	$1.87 \times 10^{-4}$
B15-WH07	5000	$2.86 \times 10^{-4}$
B20-WH07	6000	$3.55 \times 10^{-4}$
B25-WH07	8000	$3.49 \times 10^{-4}$



# COMPARING TO 1D

Until we can replace 1D CCSN models in all of their applications, we can use the 2D models to identify **areas of concern**.

Intermediate mass elements, up to  $A=50$ , are **similar**, though significant isotopic differences exist.



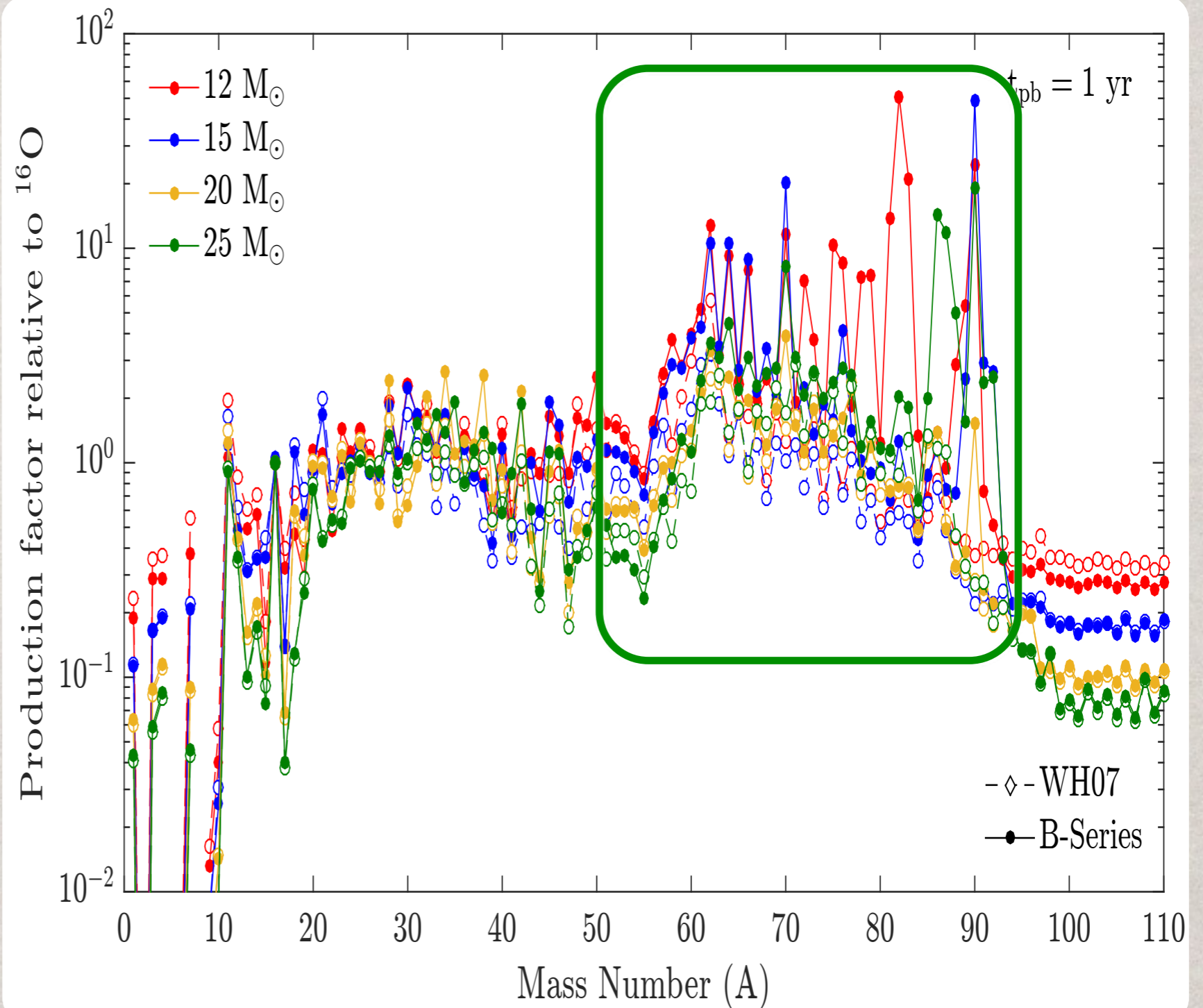


# COMPARING TO 1D

Until we can replace 1D CCSN models in all of their applications, we can use the 2D models to identify **areas of concern**.

Intermediate mass elements, up to  $A=50$ , are **similar**, though significant isotopic differences exist.

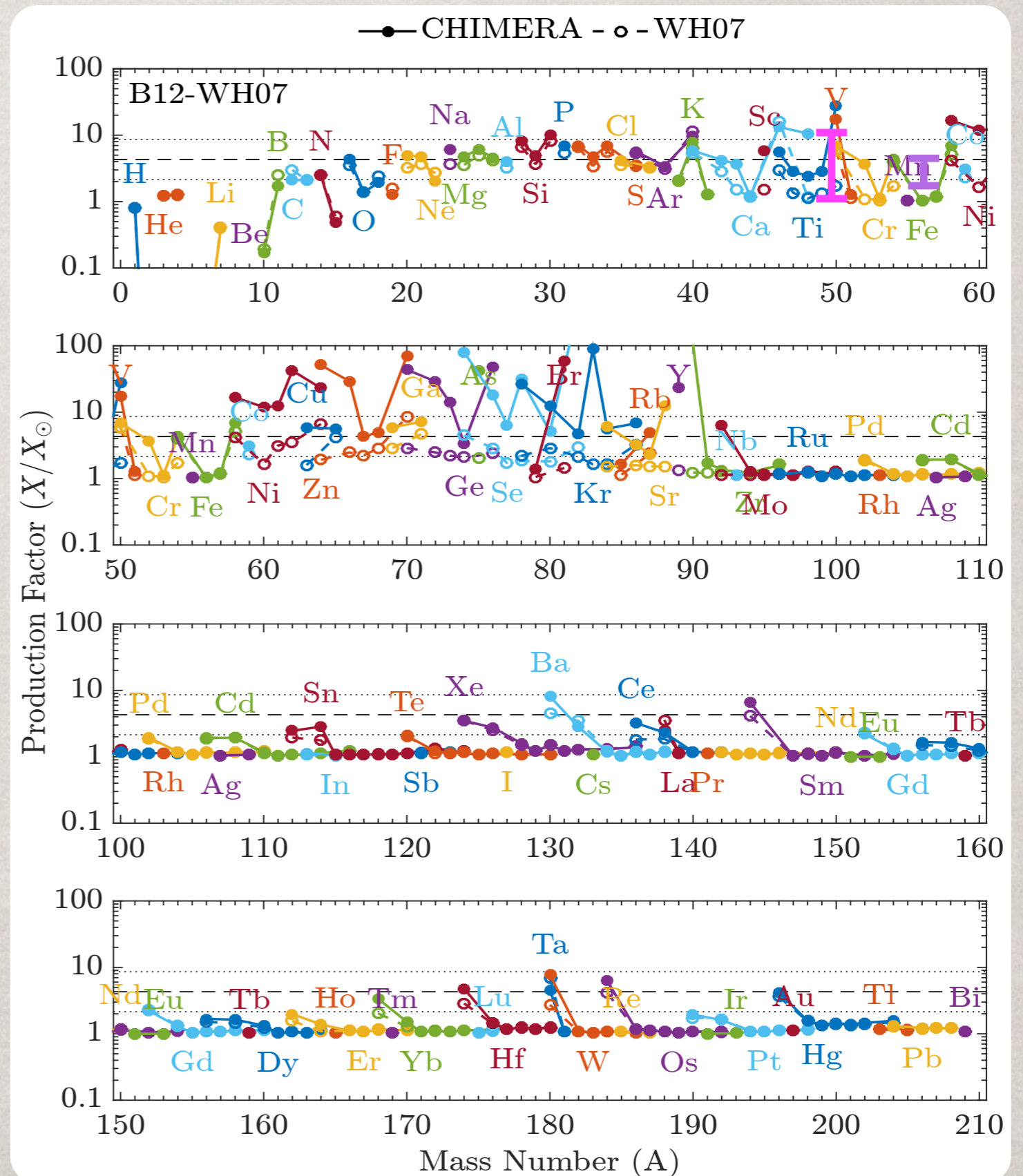
**Iron peak and heavier**, up to  $A=90$ , the **differences get larger**.



# ISOTOPIIC COMPARISON

Isotopic comparisons reveal significant differences from 1D on both the proton-rich and neutron-rich sides.

Ejection of small quantities of neutron-rich, ( $Y_e < 0.45$ ), low entropy matter produces significant amounts of neutron-rich intermediate mass isotopes like  $^{48}\text{Ca}$  and  $^{54}\text{Cr}$ .

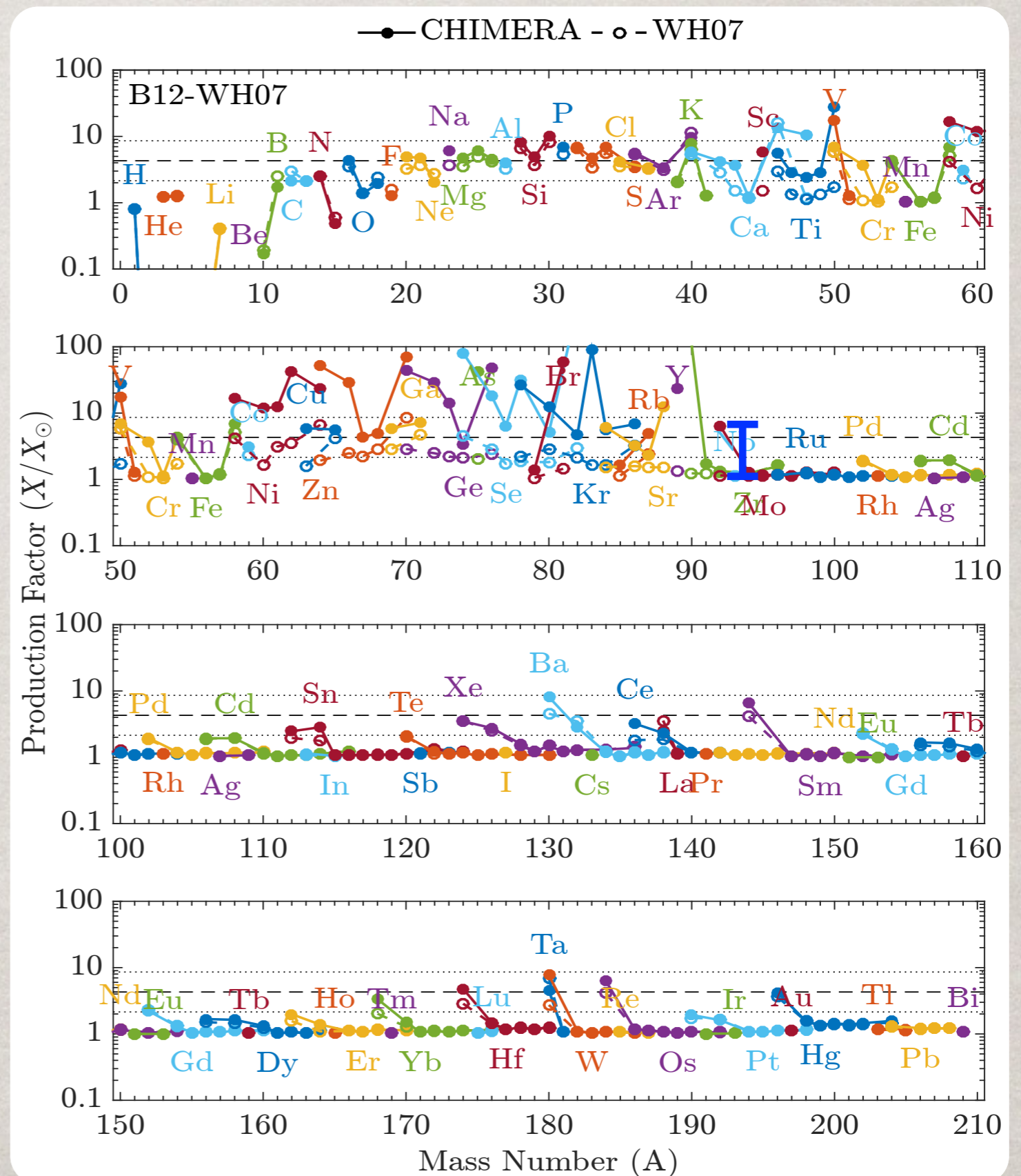


# ISOTOPIIC COMPARISON

Isotopic comparisons reveal significant differences from 1D on both the proton-rich and neutron-rich sides.

Ejection of small quantities of neutron-rich, ( $Y_e < 0.45$ ), low entropy matter produces significant amounts of neutron-rich intermediate mass isotopes like  $^{48}\text{Ca}$  and  $^{54}\text{Cr}$ .

Ejecta with somewhat higher  $Y_e$  ( $< 0.48$ ) and entropy produces  $^{92}\text{Mo}$ .



# MAGIC OF $^{48}\text{Ca}$

$^{48}\text{Ca}$ , with 20 protons and 28 neutrons, is a doubly-magic nucleus.

<b>Fe45</b>	<b>Fe46</b> 20 ms 0+	<b>Fe47</b> 27 ms	<b>Fe48</b> 44 ms 0+	<b>Fe49</b> 70 ms (7/2-)	<b>Fe50</b> 150 ms 0+	<b>Fe51</b> 305 ms 5/2-	<b>Fe52</b> 8.275 s 0-	<b>Fe53</b> 8.51 m 7/2-	<b>Fe54</b> 0+	<b>Fe55</b> 2.73 y 3/2-	<b>Fe56</b> 0+	<b>Fe57</b> 1/2-	<b>Fe58</b> 0+
	ECp	ECp	ECp	ECp	ECp	EC	EC	EC	5.8	EC	91.72	2.2	0.28
<b>Mn44</b>	<b>Mn45</b>	<b>Mn46</b> 41 ms	<b>Mn47</b> 100 ms	<b>Mn48</b> 158.1 ms 4+	<b>Mn49</b> 382 ms 5/2-	<b>Mn50</b> 283.88 ms 0-	<b>Mn51</b> 46.2 m 5/2-	<b>Mn52</b> 5.591 d 6+	<b>Mn53</b> 3.74E+6 y 7/2-	<b>Mn54</b> 312.3 d 3+	<b>Mn55</b> 5/2-	<b>Mn56</b> 2.5785 h 3+	<b>Mn57</b> 85.4 s 5/2-
		ECp	ECp	ECp,EC $\alpha$	EC	EC	EC	EC	EC	EC, $\beta^-$	100	$\beta^-$	$\beta^-$
<b>Cr43</b> 21 ms (3/2+)	<b>Cr44</b> 53 ms 0+	<b>Cr45</b> 50 ms	<b>Cr46</b> 0.26 s 0+	<b>Cr47</b> 500 ms 3/2-	<b>Cr48</b> 21.56 s 0-	<b>Cr49</b> 42.3 m 5/2-	<b>Cr50</b> 1.8E+17 y 0+	<b>Cr51</b> 27.7025 d 7/2-	<b>Cr52</b> 0+	<b>Cr53</b> 3/2-	<b>Cr54</b> 0+	<b>Cr55</b> 3.497 m 3/2-	<b>Cr56</b> 5.94 m 0+
ECp,EC $\alpha$ ,...	ECp	ECp	EC	EC	EC	EC	ECEC 4.345	EC	83.789	9.501	1.365	$\beta^-$	$\beta^-$
<b>V42</b>	<b>V43</b> 800 ms (7/2-)	<b>V44</b> 90 ms (2+)	<b>V45</b> 547 ms 7/2-	<b>V46</b> 422.37 ms 0-	<b>V47</b> 32.6 m 3/2-	<b>V48</b> 15.9735 d 4+	<b>V49</b> 330 d 7/2-	<b>V50</b> 1.4E+17 y 6+	<b>V51</b> 7/2-	<b>V52</b> 3.743 m 3+	<b>V53</b> 1.61 m 7/2-	<b>V54</b> 49.8 s 3+	<b>V55</b> 2.54 s (7/2-)
	EC	EC $\alpha$ *	EC	EC	EC	EC	EC	EC, $\beta^-$ 0.250	99.750	$\beta^-$	$\beta^-$	$\beta^-$	$\beta^-$
<b>Ti41</b> 80 ms 3/2+	<b>Ti42</b> 199 ms 0+	<b>Ti43</b> 59 ms 7/2-	<b>Ti44</b> 63 y 0-	<b>Ti45</b> 184.8 m 7/2-	<b>Ti46</b> 0+	<b>Ti47</b> 5/2-	<b>Ti48</b> 0+	<b>Ti49</b> 7/2-	<b>Ti50</b> 0+	<b>Ti51</b> 5.76 m 3/2-	<b>Ti52</b> 1.7 m 0+	<b>Ti53</b> 32.7 s (3/2-)	<b>Ti54</b> 0+
ECp	EC	EC	EC	EC	8.0	7.3	73.8	5.5	5.4	$\beta^-$	$\beta^-$	$\beta^-$	0+
<b>Sc40</b> 182.3 ms 4-	<b>Sc41</b> 596.3 ms 7/2-	<b>Sc42</b> 681.3 ms 0-	<b>Sc43</b> 3.891 h 7/2-	<b>Sc44</b> 3.927 h 2+	<b>Sc45</b> 7/2-	<b>Sc46</b> 83.79 d 4+	<b>Sc47</b> 3.3492 d 7/2-	<b>Sc48</b> 43.67 h 6+	<b>Sc49</b> 57.2 m 7/2-	<b>Sc50</b> 102.5 s 5+	<b>Sc51</b> 12.4 s (7/2-)	<b>Sc52</b> 8.2 s 4+	<b>Sc53</b>
ECp,EC $\alpha$ ,...	EC	EC	EC	EC	100	$\beta^-$ *	$\beta^-$	$\beta^-$	$\beta^-$	$\beta^-$ *	$\beta^-$	$\beta^-$	
<b>Ca39</b> 859.6 ms 3/2+	<b>Ca40</b> 0+	<b>Ca41</b> 1.03E+5 y 7/2-	<b>Ca42</b> 0+	<b>Ca43</b> 7/2-	<b>Ca44</b> 0+	<b>Ca45</b> 162.61 d 7/2-	<b>Ca46</b> 0+	<b>Ca47</b> 4.536 d 7/2-	<b>Ca48</b> 6E+15 y 0+	<b>Ca49</b> 8.718 m 3/2-	<b>Ca50</b> 1.9 s 0+	<b>Ca51</b> 10.0 s (3/2-)	<b>Ca52</b> 4.6 s 0+
EC	96.941	EC	0.647	0.135	2.086	$\beta^-$	0.004	$\beta^-$	$\beta^-$ , $\beta^-$ 0.187	$\beta^-$	$\beta^-$	$\beta$ -n	$\beta^-$
<b>K38</b> 7.636 m 3-	<b>K39</b> 3/2+	<b>K40</b> 1.277E+9 y 4-	<b>K41</b> 3/2+	<b>K42</b> 12.360 h 2-	<b>K43</b> 22.3 h 3/2+	<b>K44</b> 22.13 m 2-	<b>K45</b> 17.3 m 3/2+	<b>K46</b> 10 s (2-)	<b>K47</b> 17.50 s 1/2+	<b>K48</b> 6 s (2-)	<b>K49</b> 1.26 s (3/2+)	<b>K50</b> 472 ms (0-,1,2-)	<b>K51</b> 365 ms (1/2+,3/2+)
EC	93.2581	EC, $\beta^-$ 0.0117	6.7302	$\beta^-$	$\beta^-$	$\beta^-$	$\beta^-$	$\beta^-$	$\beta^-$	$\beta$ -n	$\beta$ -n	$\beta$ -n	$\beta$ -n

Making  $^{48}\text{Ca}$  requires **neutron-rich** conditions, but if **temperature gets too high**, it will burn to form neutron-rich iron or nickel.

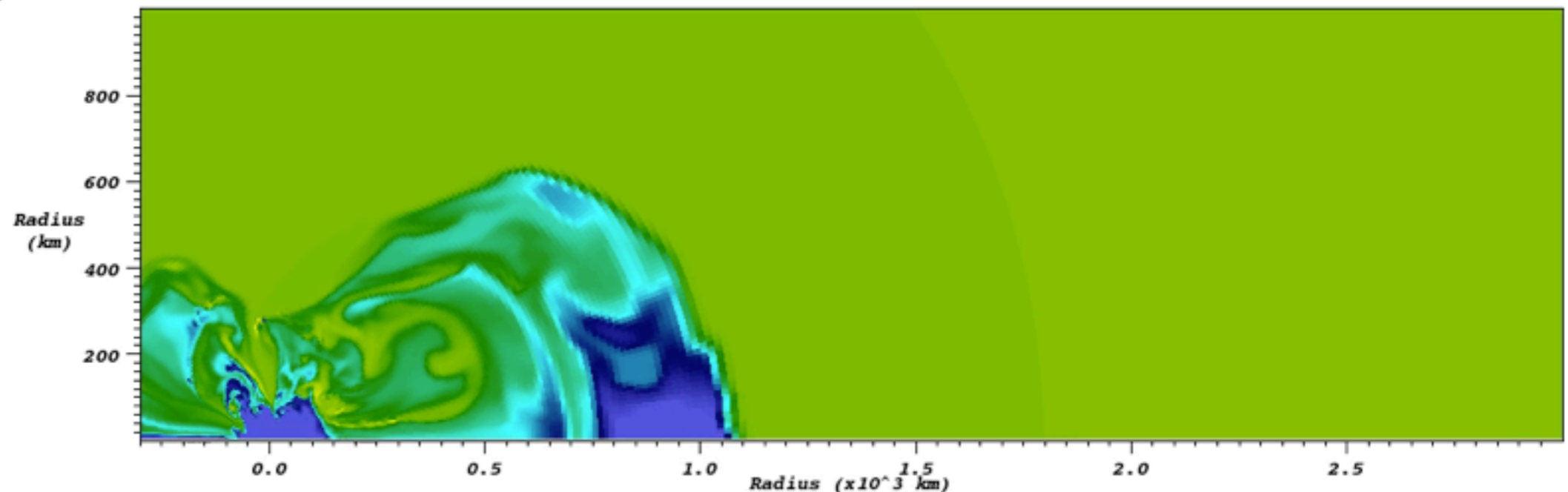
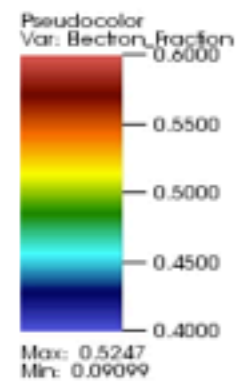
# STRIPPING A NEUTRON STAR

Relatively cold, but neutron-rich, matter is **trapped in the neutron star** and not ejected in the parameterized spherically symmetric models.

In the self-consistent, multi-dimensional models, accretion streams occasionally **dredge neutron-rich matter off the neutron-star**.

If this matter is **not heated** too much by subsequent interactions, such matter can be the source of  $^{48}\text{Ca}$ .

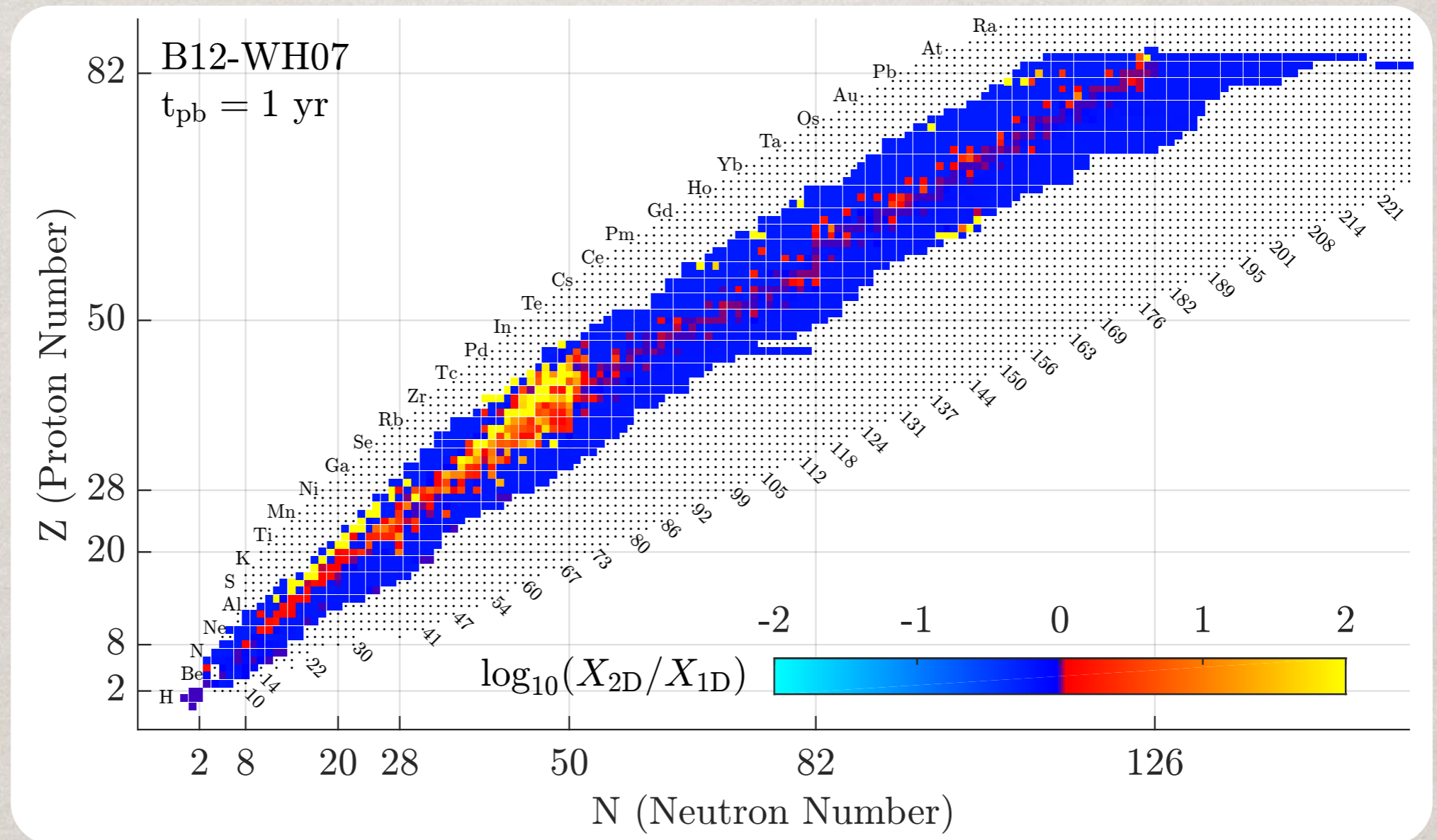
Frame 01329  
Time (elapsed) +0518.4  
Time (bounce) +0255.2



Tue May 22 04:04:02 2012

# THERMODYNAMIC VARIETY

Multi-dimensional dynamics allows the ejecta to experience a **wider variety** of temperature, density, electron fraction and neutrino exposure.



Many of these species are also seen in multi-D models of ECSN, **limiting their uniqueness as a signature.**

# CONCLUSIONS

Examining the nucleosynthesis of CCSN with models that self-consistently treat the explosion mechanism requires running the models to **times > 1 second** after bounce for uncertainties like the mass cut, thermodynamic extrapolation, etc. to become tractable.

Even then, **low post-processing resolution** is a significant uncertainty.

Differences from 1D models are seen in differing amounts of iron peak and intermediate mass elements as a result of changes in the **explosion timing** and **mass cut**.

The ejection of significantly more **proton-rich matter** as well as small quantities of **neutron-rich matter** can change the production of individual isotopes by orders of magnitude.

There is **considerable commonality** in the production of species from NSE freezeout between lower mass CCSN and ECSN. This may limit the uniqueness of some proposed ECSN signatures.

# PEEK AT THE FUTURE

DB: d9.6-2d-00329.silo

Cycle: 0

Time: 0.363247

Z9.6 2D sn160

